

Fuzzy-based Robust Precision Consensus Tracking for Uncertain Networked Systems with Cooperative-Antagonistic Interactions

Amorey Lewis

Abstract—In bipartite consensus tracking (BCT) tasks for nonlinear multiagent systems, stochastic disturbances and actuator faults are regarded as essential factors that hamper effective controller formulation and tracking precision improvement. To address these difficulties, we design an improved finite-time performance function (FTPF) for a fuzzy fault-tolerant distributed cooperative control scheme to achieve finite-time robust precision BCT tasks for nonlinear multiagent systems. The parameter selection range of the improved FTPF is relaxed, which renders systems to achieve better transient performance. Benefitting from stochastic Lyapunov stability theory, it is shown that all signals of systems are semi-global uniformly ultimately bounded in probability, and bipartite consensus errors can satisfy the arbitrary precision with probability in the predefined time. Finally, to verify its effectiveness, the proposed control scheme is applied to BCT tasks of a group of vehicles, which manifests anticipated control performance under various uncertainties.

Index Terms—Fuzzy fault-tolerant control, bipartite consensus tracking, distributed cooperative control, multiagent systems.

I. INTRODUCTION

IN the past few years, the research concerning cooperative control for multiagent systems (MASs) has attracted considerable attention due to its numerous potential applications in many fields. As a primary research topic of cooperative control, consensus requires some control variables (such as displacement and velocity) of a group of agents to reach an agreement. Following this requirement, the works [1]–[4] have proposed various control schemes to achieve the consensus of MASs. To name a few, Valcher *et al.* [1] presented a consensus control approach for homogeneous MASs with switching communication topology. According to the Internal Model Principle, a consensus control scheme for heterogeneous MASs suffering from input constraints was proposed in [2].

A common feature of the above consensus schemes is that they are designed through interactive cooperation among agents. In other words, in consensus results [1]–[4], topologies describing communications among agents exist only with non-negative edge weights. However, it is undeniable that antagonistic relations exist in some real-world scenarios. For instance, in a two-party political system, two parties may be antagonistic due to disagreements. Inspired by this fact, the bipartite consensus tracking (BCT) problem was investigated in works [5]–[9], which demands that all agents agree on some variables with the same modulus but different signs. For instance, Wen *et al.* [5] investigated the distributed BCT problem for linear MASs with a dynamic leader. In [6], the BCT problem for second-order MASs was studied, and the time of bipartite convergence can be predefined. Since stochastic disturbances are hard to avoid in the practical environment, numerous BCT results for stochastic MASs were presented in [10]–[12]. For example, Wu *et al.* [10] proposed a finite-time bipartite consensus protocol for stochastic MASs. The BCT problem for stochastic MASs with input saturation was investigated in work [11]. However, the above BCT results were obtained with actuators in normal operation. In fact, this situation may not be satisfied during systems operation. As an essential part of systems, actuators may undergo faults due to electromagnetic interference or air turbulence [13]. Actuator faults may have a detrimental effect on the tracking performance of MASs. It may even render desired control objectives challenging to achieve. In such a case, it may be hard to complete precise BCT tasks by exploiting existing control methods, especially for MASs subjected to stochastic disturbances.

As an optimization-based control approach, the prescribed performance control (PPC) in [14]–[20] has attracted considerable attention due to its ability to improve system performance. For instance, in [14], the tracking error of the considered system was constrained within specified boundaries by utilizing the PPC approach. Of note is that the above results [14]–[20] primarily focus on the steady-state performance of the system. Nevertheless, in some practical engineering [21]–[23], such as in the attitude tracking mission for the rigid spacecraft, the transient performance of attitude tracking is also critical, such that the rigid spacecraft can track a predefined attitude trajectory in a short time. In such a case, the finite-time performance function (FTPF) has been proposed in [24]–[28] to improve the convergence time of the conventional PPC method. To name a few, by designing an exponential FTPF,

Liu *et al.* [25] investigated the tracking control problem for non-strict feedback systems with the finite-time prescribed performance. In [26], a fault-tolerant tracking control strategy based on the FTPF was proposed for a class of strict feedback systems. However, it should be emphasized that the parameter selection range of the FTPF in [25]–[28] is tight, which hinders the application of FTPF, and it is even challenging to ensure that the system achieves the desired performance. Therefore, how to relax the parameter selection range and develop a fuzzy fault-tolerant distributed cooperative control scheme based on the FTPF to achieve finite-time robust precision BCT tasks for stochastic nonlinear MASs, which motivates the current research.

In this paper, the finite-time robust precision BCT problem is considered for stochastic nonlinear MASs subjected to actuator faults. The main contributions are listed as follows:

- 1) Different from existing finite-time BCT instances [8]–[10], the prescribed settling time for bipartite consensus errors is independent of the parameters of controllers and the initial states of MASs, which allows the settling time to be directly preset based on tasks requirements.
- 2) An improved FTPF is designed to program bipartite consensus errors of MASs. Compared to the existing results [25]–[28], the parameter selection range of the designed FTPF is relaxed, which enables systems to achieve better transient performance.
- 3) The proposed distributed fault-tolerant control scheme suppresses the influence of actuator faults and assorted uncertainties on systems performance while avoiding the over-parameterization problem in adaptive control methods, thereby improving the robustness of systems and reducing the redundancy of controller parameters.

The rest of this paper is organized as follows: Section II presents some preliminary knowledge, including the construction of the new FTPF. Section III shows the problem formulation for BCT tasks of stochastic MASs suffering from actuator faults. The designed procedure for the fault-tolerant controller is presented in Section IV. The stability analysis process is presented in Section V. Section VI provides simulation results of BCT tasks for second-order stochastic MASs and a group of vehicles. Conclusions of this paper can get in Section VII.

Notations: In this paper, R^n and $R^{n \times r}$ represent the n -dimensional real space and the $n \times r$ real matrix space, respectively. $\mathbf{0}$ denotes a zero matrix with appropriate dimensions. \emptyset is the empty set. For a real number ψ , $|\psi|$ denotes its absolute value. For a vector v , $\|v\|$ denotes its Euclidean norm. e is the natural constant. $\text{sgn}(\cdot)$ is a signum function. $\tanh(\cdot)$ denotes the hyperbolic tangent function. \mathcal{C}^2 denotes the set of all functions with continuous second partial derivatives. If there exists a continuous and strictly increasing function $\bar{\alpha}(x)$ that satisfies the conditions $\bar{\alpha}(0) = 0$ and $\lim_{x \rightarrow +\infty} \bar{\alpha}(x) = +\infty$, then the function $\bar{\alpha}(x)$ is called the K_∞ function.

II. PRELIMINARY KNOWLEDGE

A. Graph Theory

A signed digraph $\mathcal{G} = \{\mathbb{V}, \mathbb{E}, A\}$ is used to describe communication relationships among agents, where $\mathbb{V} =$

$\{v_1, v_2, \dots, v_N\}$ denotes the set of nodes, $\mathbb{E} \subseteq \mathbb{V} \times \mathbb{V} = \{(v_m, v_i) : v_m, v_i \in \mathbb{V}\}$ represents the set of edges, and $A = [a_{im}] \in R^{N \times N}$ is the weighted matrix with signed weights such that $a_{im} \neq 0 \Leftrightarrow (v_m, v_i) \in \mathbb{E}$ and $a_{im} = 0$, otherwise. Specifically, the edge (v_m, v_i) means that the i -th agent can receive information from the m -th agent, and the m -th agent is said to be a neighbor of the i -th agent. If the weight $a_{im} > 0$, then there is a cooperative relationship between agents i and m . Conversely, if the weight $a_{im} < 0$, this indicates an antagonistic relationship between agents i and m . In this paper, suppose that the digraph \mathcal{G} has no self-loops (i.e., $a_{ii} = 0$ or $(v_i, v_i) \notin \mathbb{E}, i = 1, \dots, N$). $L_{\mathcal{G}} = D - A$ denotes the Laplacian matrix of the digraph \mathcal{G} , where $D = \text{diag}\{\sum_{m=1}^N |a_{1m}|, \dots, \sum_{m=1}^N |a_{Nm}|\}$ denotes the in-degree matrix. If a particular node v_i can connect each node in the set of nodes \mathbb{V} through directed paths, the digraph \mathcal{G} contains a spanning tree. The particular node v_i is said to be the root of the spanning tree.

In MASs, the leader unidirectionally transmits information to followers. In the communication topology of MASs, b_i represents the weight between the i -th follower and the leader. Moreover, define the diagonal matrix $B_{\mathcal{G}} = \text{diag}\{|b_1|, \dots, |b_N|\}$, where $b_i \neq 0$ if the i -th follower can communicate directly with the leader. Otherwise, $b_i = 0$. In this paper, the leader signal and its first derivative are bounded and they can be received by followers.

Definition 1: [5] The signed digraph \mathcal{G} is called structurally balanced if the set of nodes \mathbb{V} can provide a partition $\{\mathbb{V}_1, \mathbb{V}_2\}$ satisfying conditions $\mathbb{V}_1 \cup \mathbb{V}_2 = \mathbb{V}$ and $\mathbb{V}_1 \cap \mathbb{V}_2 = \emptyset$. Moreover, if nodes v_i and v_m exist in the same subset \mathbb{V}_1 or \mathbb{V}_2 , then $a_{im} > 0$. Otherwise, $a_{im} < 0$.

Assumption 1: The considered communication topology of MASs contains a spanning tree, and the leader is the root of the spanning tree. Meanwhile, the communication topology is structurally balanced.

Lemma 1: [11] Under Assumption 1, the matrix $(L_{\mathcal{G}} + B_{\mathcal{G}})$ is nonsingular.

Lemma 2: [5] Define a set of diagonal matrices $\tilde{S} = \{S = \text{diag}\{\mathfrak{S}_1, \mathfrak{S}_2, \dots, \mathfrak{S}_N\}, \mathfrak{S}_i \in \{\pm 1\}\}$. If Assumption 1 is valid, then there exists a matrix $S \in \tilde{S}$ such that the matrix SA has all nonnegative entries. Moreover, the matrix S gives a partition, i.e. $\mathbb{V}_1 = \{v_i | \mathfrak{S}_i > 0\}$ and $\mathbb{V}_2 = \{v_i | \mathfrak{S}_i < 0\}$.

B. Stochastic Stability Theorem

The considered stochastic system is modeled as the following Itô-type stochastic differential equation:

$$dx = f(x)dt + g(x)d\varpi \quad (1)$$

where the vector $x \in R^n$ represents the system state, and $\varpi \in R^r$ denotes an independent standard Brownian motion. The functions $f(\cdot) : R^n \rightarrow R^n$ and $g(\cdot) : R^n \rightarrow R^{n \times r}$ satisfy the local Lipschitz condition with $f(\mathbf{0}) = \mathbf{0}$ and $g(\mathbf{0}) = \mathbf{0}$.

Definition 2: [29] For the system (1), if there exists a Lyapunov function $V(x) \in \mathcal{C}^2$, then the infinitesimal generator \mathcal{L} of the function $V(x)$ is defined as

$$\mathcal{L}V(x) = \frac{\partial V(x)}{\partial x} f(x) + \frac{1}{2} \text{Tr}\{G\}$$

where $G = g^T(x) \frac{\partial^2 V(x)}{\partial x^2} g(x)$, and $\text{Tr}\{G\}$ represents the trace of the matrix G .

Lemma 3: [11] It is assumed that there exists a Lyapunov function $V(x) \in \mathcal{C}^2$ satisfying the following relationships

$$\begin{aligned} \mathcal{H}_1(\|x\|) &\leq V(x) \leq \mathcal{H}_2(\|x\|) \\ \mathcal{L}V(x) &\leq -\kappa_1 V(x) + \kappa_2 \end{aligned}$$

where $\mathcal{H}_1(\|x\|)$ and $\mathcal{H}_2(\|x\|)$ belong to the K_∞ function. κ_1 and κ_2 are positive constants. Then the stochastic system (1) is said to be semi-global uniformly ultimately bounded (SGUUB) in probability. Moreover, the solution of Eq. (1) satisfies the following condition

$$E[V(x)] \leq V(x(0))e^{-\kappa_1 t} + \frac{\kappa_2}{\kappa_1}, \quad \forall t > 0$$

where $x(0)$ is the initial state, and $E(\cdot)$ represents the mathematical expectation.

C. Finite-Time Performance Function

Definition 3: [30] A function $\sigma(t)$ is said to be an FTPF if the function $\sigma(t)$ possesses the following properties

1. $\sigma(t)$ is a smooth function.
2. For $\forall t > 0$, $\sigma(t)$ satisfies $\sigma(t) > 0$ and $\dot{\sigma}(t) \leq 0$.
3. $\lim_{t \rightarrow T_s} \sigma(t) = \sigma_\infty > 0$, where σ_∞ is a constant.
4. For $\forall t \geq T_s$, $\sigma(t) = \sigma_\infty$, where T_s is the settling time.

Lemma 4: For the given constants $\varsigma \geq 1$ and $\sigma_0 > \sigma_\infty > 0$, the following segmentation function is an FTPF.

$$\sigma(t) = \begin{cases} (\sigma_0 - \sigma_\infty)e^{\varsigma(1 - \frac{T_s}{T_s - t})} + \sigma_\infty, & 0 \leq t < T_s \\ \sigma_\infty, & t \geq T_s \end{cases}$$

where T_s represents the settling time, and it depicts the convergence rate of the FTPF. Moreover, σ_∞ can be arbitrarily small, and it denotes the ultimate boundary of the FTPF.

Proof: Firstly, we give the proof of the first property.

Case 1: If $t \geq T_s$, then $\frac{d^\tau \sigma(t)}{dt^\tau} = 0$ with $\tau \geq 1$. Therefore, it is easily determined that $\frac{d^\tau \sigma(t)}{dt^\tau}$ are continuous and $\lim_{t \rightarrow T_s^+} \frac{d^\tau \sigma(t)}{dt^\tau} = 0$.

Case 2: If $0 \leq t < T_s$, then $\sigma(t) = (\sigma_0 - \sigma_\infty)e^{\alpha(t)} + \sigma_\infty$, where $\alpha(t) = \varsigma(1 - \frac{T_s}{T_s - t}) = \frac{\varsigma t}{t - T_s}$.

Taking the first-order derivative of $\sigma(t)$ with respect to time t , we can obtain

$$\frac{d\sigma(t)}{dt} = (\sigma_0 - \sigma_\infty) \frac{d\alpha(t)}{dt} e^{\alpha(t)} \quad (2)$$

where $\frac{d\alpha(t)}{dt} = \frac{-\varsigma T_s}{(t - T_s)^2}$. With the help of the L'Hospital's rule, it is not difficult to obtain

$$\begin{aligned} &\lim_{t \rightarrow T_s^-} (\sigma_0 - \sigma_\infty) \frac{d\alpha(t)}{dt} e^{\alpha(t)} \\ &= \lim_{t \rightarrow T_s^-} (\sigma_0 - \sigma_\infty) \left[\frac{-\frac{2}{\varsigma T_s}}{e^{-\frac{\varsigma t}{t - T_s}}} \right] = 0. \end{aligned} \quad (3)$$

Based on Case 1, Eqs. (2) and (3), it is derived that

$$\lim_{t \rightarrow T_s^+} \frac{d\sigma(t)}{dt} = \lim_{t \rightarrow T_s^-} \frac{d\sigma(t)}{dt} = 0$$

which indicates that the function $\frac{d\sigma(t)}{dt}$ is continuous, and $\sigma(t)$ is differentiable.

Based on Eq. (2), the second-order derivative of $\sigma(t)$ with respect to time t can be further obtained by

$$\frac{d^2 \sigma(t)}{dt^2} = (\sigma_0 - \sigma_\infty) \left[\frac{d^2 \alpha(t)}{dt^2} e^{\alpha(t)} + \left(\frac{d\alpha(t)}{dt} \right)^2 e^{\alpha(t)} \right]. \quad (4)$$

By applying the L'Hospital's rule, it yields

$$\begin{aligned} &\lim_{t \rightarrow T_s^-} (\sigma_0 - \sigma_\infty) \frac{d^2 \alpha(t)}{dt^2} e^{\alpha(t)} \\ &= \lim_{t \rightarrow T_s^-} (\sigma_0 - \sigma_\infty) \left[\frac{-\frac{6}{(t - T_s)^3}}{e^{-\frac{\varsigma t}{t - T_s}}} \right] = 0. \end{aligned} \quad (5)$$

In addition, it can also derived that

$$\begin{aligned} &\lim_{t \rightarrow T_s^-} (\sigma_0 - \sigma_\infty) \left(\frac{d\alpha(t)}{dt} \right)^2 e^{\alpha(t)} \\ &= \lim_{t \rightarrow T_s^-} (\sigma_0 - \sigma_\infty) \left[\frac{-\frac{4\varsigma T_s}{(t - T_s)^3}}{e^{-\frac{\varsigma t}{t - T_s}}} \right] = 0. \end{aligned} \quad (6)$$

Based on Case 1, and Eqs. (4)-(6), one gets

$$\lim_{t \rightarrow T_s^+} \frac{d^2 \sigma(t)}{dt^2} = \lim_{t \rightarrow T_s^-} \frac{d^2 \sigma(t)}{dt^2} = 0$$

which indicates that $\frac{d^2 \sigma(t)}{dt^2}$ is continuous, and $\sigma(t)$ being the second-order differentiable.

Based on the above analysis, it can deduce that $\frac{d^\tau \sigma(t)}{dt^\tau} = \frac{\hat{\gamma}_\tau}{(t - T_s)^{\tau+1}}$ and $\left(\frac{d\alpha(t)}{dt} \right)^\tau = \frac{\check{\gamma}_\tau}{(t - T_s)^{2\tau}}$, where $\hat{\gamma}_\tau$ and $\check{\gamma}_\tau$ are constants, and $3 \leq \tau \leq n-1$. Therefore, $\frac{d^\tau \sigma(t)}{dt^\tau}$ can be denoted as a polynomial of $\frac{e^{\alpha(t)}}{(t - T_s)^m}$ with $m \geq 0$.

Through the above analysis, it can be obtained

$$\begin{aligned} &\lim_{t \rightarrow T_s^-} \left[\frac{e^{\alpha(t)}}{(t - T_s)^m} \right] = -\frac{m}{\varsigma T_s} \lim_{t \rightarrow T_s^-} \left[\frac{\frac{1}{(t - T_s)^{m-1}}}{e^{-\frac{\varsigma t}{t - T_s}}} \right] \\ &\dots \\ &= (-1)^{(m+1)} \frac{\prod_{j=0}^{(m-1)} (m-j)}{(\varsigma T_s)^{(m-1)}} \lim_{t \rightarrow T_s^-} \left[\frac{\frac{1}{t - T_s}}{e^{-\frac{\varsigma t}{t - T_s}}} \right] = 0. \end{aligned} \quad (7)$$

According to Case 1 and (7), it follows that

$$\lim_{t \rightarrow T_s^-} \left[\frac{d^\tau \sigma(t)}{dt^\tau} \right] = \lim_{t \rightarrow T_s^+} \left[\frac{d^\tau \sigma(t)}{dt^\tau} \right] = 0$$

which means that $\frac{d^\tau \sigma(t)}{dt^\tau}$ is continuous, and $\sigma(t)$ is τ -times differentiable.

At last, by taking $\tau = n$, it yields

$$\lim_{t \rightarrow T_s^-} \left[\frac{d^n \sigma(t)}{dt^n} \right] = 0.$$

It should notice that

$$\lim_{t \rightarrow T_s^-} \left[\frac{d^n \sigma(t)}{dt^n} \right] = \lim_{t \rightarrow T_s^+} \left[\frac{d^n \sigma(t)}{dt^n} \right] = 0$$

which indicates that $\frac{d^n \sigma(t)}{dt^n}$ is continuous, and $\sigma(t)$ is n -times differentiable.

The above analysis can conclude that the function $\sigma(t)$ satisfies the first property. Furthermore, it is not difficult to verify that $\sigma(t)$ satisfies other properties. According to Definition 3, $\sigma(t)$ is an FTPF.

This completes the proof. \blacksquare

Remark 1: In [25]–[28], the parameter selection range of the FTPF is tight, which hampers the application of FTPF, and it is even hard to guarantee that MASs achieve the desired performance. Compared to the existing results [25]–[28], the parameter selection range of the improved FTPF is relaxed, which renders systems to achieve better transient performance.

D. Fuzzy Logic System

The fuzzy logic system (FLS) has excellent approximation ability to the unknown nonlinear function. The conventional fuzzy rules are as follows:

R^l : If x_1 is F_1^l, \dots , and x_n is F_n^l , then y_F is W^l .

Specifically, $x = [x_1, \dots, x_n]^T$ and y_F are input and output of the FLS, respectively. F_j^l and W^l are fuzzy sets with membership functions $\phi_{F_j^l}(x_j)$ and $\phi_{W^l}(x_j)$, where $j = 1, 2, \dots, n$ and $l = 1, 2, \dots, P$. Based on the results in [31]–[39], the output y_F of the FLS can be written as

$$y_F(x) = \frac{\sum_{l=1}^P \bar{y}_F^l \left[\prod_{j=1}^n \phi_{F_j^l}(x_j) \right]}{\sum_{l=1}^P \left[\prod_{j=1}^n \phi_{F_j^l}(x_j) \right]} \quad (8)$$

where $\bar{y}_F^l = \max_{y_F \in R} \{\phi_{W^l}(y_F)\}$. The fuzzy basis function can be represented by

$$\Phi_l(x) = \frac{\prod_{j=1}^n \phi_{F_j^l}(x_j)}{\sum_{l=1}^P \left[\prod_{j=1}^n \phi_{F_j^l}(x_j) \right]}.$$

Denote $\theta = [\bar{y}_F^1, \bar{y}_F^2, \dots, \bar{y}_F^P]^T = [\theta_1, \theta_2, \dots, \theta_P]^T$ and $\Phi(x) = [\Phi_1(x), \Phi_2(x), \dots, \Phi_P(x)]^T$. Eq. (8) can be further written as

$$y_F(x) = \theta^T \Phi(x).$$

Lemma 5: [40] If $r(x)$ is a continuous function defined on a compact set Ω_r , then there exists an FLS $\theta^T \Phi(x)$ satisfying the following relationship

$$\sup_{x \in \Omega_r} |r(x) - \theta^T \Phi(x)| \leq \epsilon_r$$

where ϵ_r is any positive constant.

III. PROBLEM FORMULATION

In this paper, the i -th follower is modeled as

$$\begin{cases} dx_{ij} = (x_{i(j \bullet 1)} + f_{ij}(\bar{x}_{ij})) dt + g_{ij}(\bar{x}_{ij}) d\varpi \\ dx_{in_i} = \left(\sum_{h=1}^M l_{ih} \omega_{ih} + f_{in_i}(\bar{x}_{in_i}) \right) dt + g_{in_i}(\bar{x}_{in_i}) d\varpi \\ y_i = x_{i1}, \quad 1 \leq i \leq N, \quad 1 \leq j \leq n_i - 1 \end{cases} \quad (9)$$

where $\bar{x}_{i\ell} = [x_{i1}, x_{i2}, \dots, x_{i\ell}]^T$ ($\ell = 1, 2, \dots, n_i$) and $y_i \in R$ represent the state variables and output of the i -th follower, respectively. $f_{i\ell}(\cdot) : R^\ell \rightarrow R$ and $g_{i\ell}(\cdot) : R^\ell \rightarrow R^{1 \times r}$ denote unknown nonlinear functions satisfying the local Lipschitz condition. $f_{i\ell}(\mathbf{0}) = 0$ and $g_{i\ell}(\mathbf{0}) = \mathbf{0}$. $l_{ih} \in R$ is an unknown

coefficient. ω_{ih} denotes the output of the h -th actuator of the i -th follower. M represents the number of the actuator. ϖ is an independent r -dimensional standard Brownian motion, which is defined on a complete probability space $(\Omega, \mathcal{F}, \{\mathcal{F}_t\}_{t \geq 0}, \bar{P})$. $\bar{\Omega}$ stands for a sample space. \mathcal{F} denotes a $\bar{\sigma}$ -field. $\{\mathcal{F}_t\}_{t \geq 0}$ represents a filtration, and \bar{P} is a probability measure. In the subsequent derivation, for simplicity, functions $f_{i\ell}(\bar{x}_{i\ell})$ and $g_{i\ell}(\bar{x}_{i\ell})$ concerning states variables $\bar{x}_{i\ell}$ will be denoted by $f_{i\ell}$ and $g_{i\ell}$, respectively.

The actuator fault model is described by

$$\begin{cases} \omega_{ih}(t) = \rho_{ih} u_{ih}(t) + \nu_{ih}, & t \in [t_{ih}^s, t_{ih}^e) \\ \rho_{ih} \nu_{ih} = 0, & \iota = 1, 2, 3, \dots \end{cases} \quad (10)$$

where $\rho_{ih} \in [0, 1]$ and ν_{ih} are unknown constants. $u_{ih}(t)$ is the input of the h -th actuator of the i -th follower. ι indicates the ι -th actuator fault. t_{ih}^s and t_{ih}^e represent the moments when the fault occurs and ends, respectively. Eq. (10) involves the following three situations:

- If $\rho_{ih} = 1$ and $\nu_{ih} = 0$, then actuators work normally.
- For unknown constants $\underline{\rho}_{ih}$ and $\bar{\rho}_{ih}$, if $0 < \underline{\rho}_{ih} \leq \rho_{ih} \leq \bar{\rho}_{ih} < 1$ and $\nu_{ih} = 0$, then actuators undergo the partial loss of control effectiveness (PLOE).
- If $\rho_{ih} = 0$ and $\nu_{ih} \neq 0$, then actuators occur the total loss of effectiveness (TLOE).

Control Objectives: This paper aims at developing an FTPF-based control scheme for stochastic MASs to complete the following control objectives:

- All signals of MASs are SGUUB in probability.
- Bipartite consensus errors satisfy the arbitrary precision with probability in the predefined settling time.

Other assumptions and lemmas need to be provided to guarantee that control objectives are achieved.

Assumption 2: Only up to $M - 1$ actuators are allowed to work in the TLOE mode.

Assumption 3: For the dynamics model of the i -th follower, the signs of l_{ih} ($h = 1, 2, \dots, M$) are known.

Lemma 6: [11] (Young's inequality): For $\forall \mathcal{P} \in R^n, \forall \mathcal{Q} \in R^n$, the following relationship holds

$$\mathcal{P}\mathcal{Q} \leq \frac{\varepsilon^{c_1}}{c_1} |\mathcal{P}|^{c_1} + \frac{1}{c_2 \varepsilon^{c_2}} |\mathcal{Q}|^{c_2}$$

where $c_1 > 1, c_2 > 1, \varepsilon > 0$, and $\frac{1}{c_1} + \frac{1}{c_2} = 1$.

Lemma 7: [41] For any given variable Ξ , one has

$$0 \leq |\Xi| - \frac{\Xi^2}{\sqrt{\Xi^2 + \psi^2}} \leq \psi$$

where ψ is a positive constant.

IV. FAULT-TOLERANT CONTROLLER DESIGN

A. Error Transformation

To achieve the control objective (b), the error transformation mechanism in [42] is adopted. Before giving the error transformation mechanism, the bipartite consensus error z_{i1} is defined as

$$z_{i1} = \sum_{m=1}^N |a_{im}| (y_i - \text{sgn}(a_{im}) y_m) + |b_i| (y_i - \text{sgn}(b_i) y_r) \quad (11)$$

where y_r denotes the leader signal.

The error transformation mechanism is given as

$$z_{i1} = \sigma(t)\mu(e_{i1}^*), \quad |z_{i1}(0)| \in (0, \sigma(0)) \quad (12)$$

where $\mu(e_{i1}^*) = \frac{2}{\pi} \arctan(e_{i1}^*)$, and e_{i1}^* is the transformed error. Based on Eq. (12) and the fourth property of the FTF, for $\forall t \geq T_s$, one gets

$$-\sigma_\infty < z_{i1} < \sigma_\infty \quad (13)$$

which indicates that the bipartite consensus error z_{i1} can converge to a predefined region in a finite time T_s . In the subsequent coordinate transformations, e_{i1}^* will replace z_{i1} to participate in the construction of the controller.

By taking the differential of Eqs. (11) and (12), one obtains

$$\begin{aligned} dz_{i1} &= \mu(e_{i1}^*)d\sigma(t) + \sigma(t)\frac{\partial\mu(e_{i1}^*)}{\partial e_{i1}^*}de_{i1}^* \\ &= \left(q_i(x_{i2} + f_{i1}) - \sum_{m=1}^N a_{im}(x_{m2} + f_{m1}) - b_i\dot{y}_r\right)dt \\ &\quad + \left(q_i g_{i1} - \sum_{m=1}^N a_{im}g_{m1}\right)d\tau \end{aligned} \quad (14)$$

with $q_i = \sum_{m=1}^N |a_{im}| + |b_i|$.

Furthermore, it follows that

$$\begin{aligned} de_{i1}^* &= \xi_i \left(q_i(x_{i2} + f_{i1}) - \sum_{m=1}^N a_{im}(x_{m2} + f_{m1}) - b_i\dot{y}_r - \beta_i \right) dt \\ &\quad + \xi_i \left(q_i g_{i1} - \sum_{m=1}^N a_{im}g_{m1} \right) d\tau \end{aligned} \quad (15)$$

where $\beta_i = \frac{2}{\pi} \arctan(e_{i1}^*)\dot{\sigma}(t)$, and $\xi_i = \frac{\pi(1+e_{i1}^{*2})}{2\sigma(t)}$.

Remark 2: It is necessary to ensure that bipartite consensus error z_{i1} satisfies inequality (13) to achieve control objective (b). Therefore, the error transformation mechanism (12) is introduced to guarantee that inequality (13) holds. The mechanism (12) means that $z_{i1} \rightarrow \pm\sigma_\infty$ if and only if $e_{i1}^* \rightarrow \pm\infty$, for $\forall t \geq T_s$. Consequently, as long as e_{i1}^* is bounded, inequality (13) can be guaranteed to be true, thus ensuring that control objective (b) can be achieved.

B. Fault-Tolerant Controller Design

Before the design of the fault-tolerant controller, the coordinate transformations are provided as

$$\begin{cases} \zeta_{i1} = e_{i1}^* \\ \zeta_{ih} = x_{ih} - \alpha_{i(h-1)}^*, \quad h = 2, 3, \dots, n_i \end{cases} \quad (16)$$

where $\alpha_{i(h-1)}^*$ is the output of the first-order command filter with respect to the virtual controller $\alpha_{i(h-1)}$. $\alpha_{i(h-1)}^*$ and $\alpha_{i(h-1)}$ satisfy the following relationship

$$\tau_{i(h-1)}\dot{\alpha}_{i(h-1)}^* + \alpha_{i(h-1)}^* = \alpha_{i(h-1)}$$

where $\tau_{i(h-1)}$ is a positive designed parameter, and initial values of $\alpha_{i(h-1)}^*$ and $\alpha_{i(h-1)}$ satisfy $\alpha_{i(h-1)}^*(0) = \alpha_{i(h-1)}(0)$.

Step 1: Choose the following Lyapunov function

$$V_{i1} = \frac{1}{4}\bar{\zeta}_{i1}^4 + \frac{1}{2\delta_i}\tilde{\Theta}_i^2$$

where $\bar{\zeta}_{i1} = \zeta_{i1} - \eta_{i1}$ is a compensated error, and $\tilde{\Theta}_i = \Theta_i - \hat{\Theta}_i$. $\Theta_i \triangleq \max_{1 \leq i \leq n_i} \{\|\theta_{i1}\|^{\frac{4}{3}}, \|\theta_{i2}\|^2\}$ is an unknown constant, and $\hat{\Theta}_i$ is the estimated value of Θ_i . δ_i is a positive designed parameter. To compensate the filtering error $\alpha_{i1}^* - \alpha_{i1}$, the compensation signal η_{i1} is designed as

$$\begin{aligned} \dot{\eta}_{i1} &= -(k_{i1} + 1)\eta_{i1} + \xi_i q_i (\alpha_{i1}^* - \alpha_{i1}) + \xi_i q_i \eta_{i2} \\ &\quad - \lambda_{i1} \xi_i q_i \text{sgn}(\eta_{i1}) \end{aligned} \quad (17)$$

where k_{i1} and λ_{i1} are positive designed parameters. Based on Eqs. (15)-(17), the infinitesimal generator of V_{i1} is given as

$$\begin{aligned} \mathcal{L}V_{i1} &= \bar{\zeta}_{i1}^3 \left[\xi_i \left(q_i(\bar{\zeta}_{i2} + \alpha_{i1} + f_{i1}) - \sum_{m=1}^N a_{im}(x_{m2} + f_{m1}) - b_i\dot{y}_r \right. \right. \\ &\quad \left. \left. - \frac{2}{\pi} \arctan(e_{i1}^*)\dot{\sigma}(t) \right) + (k_{i1} + 1)\eta_{i1} + \lambda_{i1} \xi_i q_i \text{sgn}(\eta_{i1}) \right] \\ &\quad + \frac{3}{2}\bar{\zeta}_{i1}^2 \xi_i^2 \Lambda_i \Lambda_i^T - \frac{1}{\delta_i} \tilde{\Theta}_i \dot{\tilde{\Theta}}_i \end{aligned} \quad (18)$$

where $\bar{\zeta}_{i2} = \zeta_{i2} - \eta_{i2}$, and $\Lambda_i = q_i g_{i1} - \sum_{m=1}^N a_{im}g_{m1}$.

Note that f_{i1} and f_{m1} are unknown functions in Eq. (18). For the sake of subsequent derivation, we sum all terms that contain f_{i1} and f_{m1} . The result of the sum is denoted by \mathcal{F}_{i1}^* , and the expression for \mathcal{F}_{i1}^* is given as

$$\mathcal{F}_{i1}^* = f_{i1}q_i - \sum_{m=1}^N a_{im}(x_{m2} + f_{m1}).$$

To approximate unknown functions \mathcal{F}_{i1}^* and $\Lambda_i \Lambda_i^T$, FLSs $\theta_{i11}^T \Phi_{i11}(X_{i11})$ and $\theta_{i12}^T \Phi_{i12}(X_{i12})$ are utilized, respectively. For any positive constants ϵ_{i11}^* and ϵ_{i12}^* , one obtains

$$\begin{aligned} \mathcal{F}_{i1}^* &= \theta_{i11}^T \Phi_{i11}(X_{i11}) + \epsilon_{i11}(X_{i11}) \\ \Lambda_i \Lambda_i^T &= \theta_{i12}^T \Phi_{i12}(X_{i12}) + \epsilon_{i12}(X_{i12}) \end{aligned}$$

where $X_{i11} = [x_{i1}, x_{m1}, x_{m2}]^T$ and $X_{i12} = [x_{i1}, x_{m1}]^T$ ($m \neq i$). $\epsilon_{i11}(X_{i11})$ and $\epsilon_{i12}(X_{i12})$ are approximation errors, and they satisfy $\epsilon_{i11}(X_{i11}) \leq \epsilon_{i11}^*$ and $\epsilon_{i12}(X_{i12}) \leq \epsilon_{i12}^*$, respectively. Based on Lemma 6, it follows that

$$\begin{aligned} \bar{\zeta}_{i1}^3 \xi_i \mathcal{F}_{i1}^* &= \bar{\zeta}_{i1}^3 \xi_i [\theta_{i11}^T \Phi_{i11}(X_{i11}) + \epsilon_{i11}(X_{i11})] \\ &\leq \frac{3\epsilon_{i11}^{\frac{4}{3}}}{4} \bar{\zeta}_{i1}^4 \xi_i^{\frac{4}{3}} \|\theta_{i11}\|^{\frac{4}{3}} \|\Phi_{i11}\|^{\frac{4}{3}} + \frac{1}{4\epsilon_{i11}^4} \\ &\quad + \frac{3\epsilon_{i12}^{\frac{4}{3}}}{4} \bar{\zeta}_{i1}^4 \xi_i^{\frac{4}{3}} + \frac{\epsilon_{i11}^4}{4\epsilon_{i12}^4} \\ &\leq \frac{3\epsilon_{i11}^{\frac{4}{3}}}{4} \bar{\zeta}_{i1}^4 \xi_i^{\frac{4}{3}} \Theta_i \|\Phi_{i11}\|^{\frac{4}{3}} + \frac{1}{4\epsilon_{i11}^4} \\ &\quad + \frac{3\epsilon_{i12}^{\frac{4}{3}}}{4} \bar{\zeta}_{i1}^4 \xi_i^{\frac{4}{3}} + \frac{\epsilon_{i11}^4}{4\epsilon_{i12}^4} \end{aligned} \quad (19)$$

where ϵ_{i11} and ϵ_{i12} are positive designed parameters. Similar to inequality (19), the following inequality holds

$$\frac{3}{2}\bar{\zeta}_{i1}^2 \xi_i^2 \Lambda_i \Lambda_i^T = \frac{3}{2}\bar{\zeta}_{i1}^2 \xi_i^2 [\theta_{i12}^T \Phi_{i12}(X_{i12}) + \epsilon_{i12}(X_{i12})]$$

$$\begin{aligned}
&\leq \frac{3\varepsilon_{i13}^2}{4} \bar{\zeta}_{i1}^4 \xi_i^4 \|\theta_{i12}\|^2 \|\Phi_{i12}\|^2 + \frac{3}{4\varepsilon_{i13}^2} \\
&\quad + \frac{3\varepsilon_{i14}^2}{4} \bar{\zeta}_{i1}^4 \xi_i^4 + \frac{3\varepsilon_{i12}^2}{4\varepsilon_{i14}^2} \\
&\leq \frac{3\varepsilon_{i13}^2}{4} \bar{\zeta}_{i1}^4 \xi_i^4 \Theta_i \|\Phi_{i12}\|^2 + \frac{3}{4\varepsilon_{i13}^2} \\
&\quad + \frac{3\varepsilon_{i14}^2}{4} \bar{\zeta}_{i1}^4 \xi_i^4 + \frac{3\varepsilon_{i12}^2}{4\varepsilon_{i14}^2} \quad (20)
\end{aligned}$$

where ε_{i13} and ε_{i14} are positive designed parameters. By using Lemma 6, it is not difficult to derive

$$\lambda_{i1} q_i \bar{\zeta}_{i1}^3 \xi_i \text{sgn}(\eta_{i1}) \leq \frac{3}{4} \bar{\zeta}_{i1}^4 \xi_i^4 + \frac{\lambda_{i1}^4 q_i^4}{4}. \quad (21)$$

By substituting inequalities (19)-(21) to (18), one gets

$$\begin{aligned}
\mathcal{L}V_{i1} &\leq \bar{\zeta}_{i1}^3 \left[\xi_i \left(q_i (\bar{\zeta}_{i2} + \alpha_{i1}) - b_i \dot{y}_r - \frac{2}{\pi} \arctan(e_{i1}^*) \dot{\sigma}(t) \right. \right. \\
&\quad \left. \left. + \frac{k_{i1} + 1}{\xi_i} \eta_{i1} \right) + \frac{3}{4} \bar{\zeta}_{i1} \xi_i^4 + \frac{3\varepsilon_{i11}^2}{4} \bar{\zeta}_{i1} \xi_i^4 \Theta_i \|\Phi_{i11}\|^4 \right. \\
&\quad \left. + \frac{3\varepsilon_{i12}^2}{4} \bar{\zeta}_{i1} \xi_i^4 + \frac{3\varepsilon_{i13}^2}{4} \bar{\zeta}_{i1} \xi_i^4 \Theta_i \|\Phi_{i12}\|^2 + \frac{3\varepsilon_{i14}^2}{4} \bar{\zeta}_{i1} \xi_i^4 \right] \\
&\quad - \frac{1}{\delta_i} \tilde{\Theta}_i \dot{\Theta}_i + \frac{\lambda_{i1}^4 q_i^4}{4} + \frac{1}{4\varepsilon_{i11}^4} + \frac{\varepsilon_{i11}^4}{4\varepsilon_{i12}^4} + \frac{3}{4\varepsilon_{i13}^2} + \frac{3\varepsilon_{i12}^2}{4\varepsilon_{i14}^2}.
\end{aligned}$$

Then, the virtual controller α_{i1} can be designed as

$$\begin{aligned}
\alpha_{i1} &= -\frac{k_{i1} + 1}{\xi_i q_i} \bar{\zeta}_{i1} + \frac{1}{q_i} \left(b_i \dot{y}_r + \frac{2}{\pi} \arctan(e_{i1}^*) \dot{\sigma}(t) \right. \\
&\quad \left. - \frac{3\varepsilon_{i11}^2}{4} \bar{\zeta}_{i1} \xi_i^4 \tilde{\Theta}_i \|\Phi_{i11}\|^4 - \frac{3\varepsilon_{i13}^2}{4} \bar{\zeta}_{i1} \xi_i^4 \tilde{\Theta}_i \|\Phi_{i12}\|^2 \right. \\
&\quad \left. - \frac{3}{4} \bar{\zeta}_{i1} \xi_i^4 - \frac{3\varepsilon_{i12}^2}{4} \bar{\zeta}_{i1} \xi_i^4 - \frac{3\varepsilon_{i14}^2}{4} \bar{\zeta}_{i1} \xi_i^4 \right). \quad (22)
\end{aligned}$$

By substituting the virtual controller α_{i1} to $\mathcal{L}V_{i1}$, the following inequality holds

$$\mathcal{L}V_{i1} \leq \bar{\zeta}_{i1}^3 \xi_i q_i \bar{\zeta}_{i2} - (k_{i1} + 1) \bar{\zeta}_{i1}^4 + \frac{1}{\delta_i} \tilde{\Theta}_i (\Delta_{i1} - \dot{\Theta}_i) + \Upsilon_{i1}$$

where $\Delta_{i1} = \frac{3\varepsilon_{i11}^2}{4} \bar{\zeta}_{i1}^4 \xi_i^4 \|\Phi_{i11}\|^4 + \frac{3\varepsilon_{i13}^2}{4} \bar{\zeta}_{i1}^4 \xi_i^4 \|\Phi_{i12}\|^2$, and $\Upsilon_{i1} = \frac{\lambda_{i1}^4 q_i^4}{4} + \frac{1}{4\varepsilon_{i11}^4} + \frac{\varepsilon_{i11}^4}{4\varepsilon_{i12}^4} + \frac{3}{4\varepsilon_{i13}^2} + \frac{3\varepsilon_{i12}^2}{4\varepsilon_{i14}^2}$.

Step 2: Construct the following Lyapunov function

$$V_{i2} = V_{i1} + \frac{1}{4} \bar{\zeta}_{i2}^4$$

where $\bar{\zeta}_{i2} = \zeta_{i2} - \eta_{i2}$. To eliminate the filtering error $\alpha_{i2}^* - \alpha_{i2}$, the second compensation signal η_{i2} is designed as

$$\begin{aligned}
\dot{\eta}_{i2} &= -(k_{i2} + 1) \eta_{i2} + (\alpha_{i2}^* - \alpha_{i2}) - \xi_i q_i \eta_{i1} \\
&\quad + \eta_{i3} - \lambda_{i2} \text{sgn}(\eta_{i2}) \quad (23)
\end{aligned}$$

where k_{i2} and λ_{i2} are positive designed parameters.

Similar to Eq. (18), the infinitesimal generator of V_{i2} can be calculated as

$$\begin{aligned}
\mathcal{L}V_{i2} &\leq \bar{\zeta}_{i1}^3 \xi_i q_i \bar{\zeta}_{i2} - (k_{i1} + 1) \bar{\zeta}_{i1}^4 + \frac{1}{\delta_i} \tilde{\Theta}_i (\Delta_{i1} - \dot{\Theta}_i) + \Upsilon_{i1} \\
&\quad + \bar{\zeta}_{i2}^3 \left(\bar{\zeta}_{i3} + \alpha_{i2} + f_{i2} - \dot{\alpha}_{i1}^* + (k_{i2} + 1) \eta_{i2} + \xi_i q_i \eta_{i1} \right.
\end{aligned}$$

$$\left. + \lambda_{i2} \text{sgn}(\eta_{i2}) \right) + \frac{3}{2} \bar{\zeta}_{i2}^2 g_{i2} g_{i2}^T. \quad (24)$$

Note that unknown nonlinear functions f_{i2} and $g_{i2} g_{i2}^T$ exist in inequality (24). Similar to inequalities (19) and (20), we can obtain

$$\bar{\zeta}_{i2}^3 f_{i2} \leq \frac{3\varepsilon_{i21}^2}{4} \bar{\zeta}_{i2}^4 \Theta_i \|\Phi_{i21}\|^4 + \frac{1}{4\varepsilon_{i21}^4} + \frac{3\varepsilon_{i22}^2}{4} \bar{\zeta}_{i2}^4 + \frac{\varepsilon_{i21}^4}{4\varepsilon_{i22}^4}$$

where ε_{i21} and ε_{i22} are positive designed parameters, and ε_{i21}^* is any given positive constant. Moreover, we have

$$\frac{3}{2} \bar{\zeta}_{i2}^2 g_{i2} g_{i2}^T \leq \frac{3\varepsilon_{i23}^2}{4} \bar{\zeta}_{i2}^4 \Theta_i \|\Phi_{i22}\|^2 + \frac{3}{4\varepsilon_{i23}^2} + \frac{3\varepsilon_{i24}^2}{4} \bar{\zeta}_{i2}^4 + \frac{3\varepsilon_{i22}^2}{4\varepsilon_{i24}^2}$$

where ε_{i23} and ε_{i24} are positive designed parameters, and ε_{i22}^* is any given positive constant. By using Lemma 6, it is not difficult to derive

$$\begin{cases} \bar{\zeta}_{i1}^3 \xi_i q_i \bar{\zeta}_{i2} \leq \bar{\zeta}_{i1}^4 + \frac{3^3}{4} \xi_i^4 q_i^4 \bar{\zeta}_{i2}^4 \\ \bar{\zeta}_{i2}^3 \lambda_{i2} \text{sgn}(\eta_{i2}) \leq \frac{3}{4} \bar{\zeta}_{i2}^4 + \frac{\lambda_{i2}^4}{4} \end{cases}$$

According to the above results, inequality (24) can be further rewritten as

$$\begin{aligned}
\mathcal{L}V_{i2} &\leq \frac{3^3}{4} \xi_i^4 q_i^4 \bar{\zeta}_{i2}^4 - k_{i1} \bar{\zeta}_{i1}^4 + \frac{1}{\delta_i} \tilde{\Theta}_i (\Delta_{i1} - \dot{\Theta}_i) + \Upsilon_{i1} \\
&\quad + \bar{\zeta}_{i2}^3 \left(\bar{\zeta}_{i3} + \alpha_{i2} + \frac{3\varepsilon_{i21}^2}{4} \bar{\zeta}_{i2} \Theta_i \|\Phi_{i21}\|^4 + \frac{3\varepsilon_{i22}^2}{4} \bar{\zeta}_{i2} \right. \\
&\quad \left. + \frac{3\varepsilon_{i23}^2}{4} \bar{\zeta}_{i2} \Theta_i \|\Phi_{i22}\|^2 + \frac{3\varepsilon_{i24}^2}{4} \bar{\zeta}_{i2} - \dot{\alpha}_{i1}^* + \xi_i q_i \eta_{i1} \right. \\
&\quad \left. + (k_{i2} + 1) \eta_{i2} + \frac{3}{4} \bar{\zeta}_{i2} \right) + \frac{1}{4\varepsilon_{i21}^4} + \frac{\varepsilon_{i21}^4}{4\varepsilon_{i22}^4} + \frac{3}{4\varepsilon_{i23}^2} \\
&\quad + \frac{3\varepsilon_{i22}^2}{4\varepsilon_{i24}^2} + \frac{\lambda_{i2}^4}{4}. \quad (25)
\end{aligned}$$

Based on inequality (25), the virtual controller α_{i2} can be constructed as

$$\begin{aligned}
\alpha_{i2} &= -(k_{i2} + 1) \zeta_{i2} + \dot{\alpha}_{i1}^* - \frac{3\varepsilon_{i21}^2}{4} \bar{\zeta}_{i2} \tilde{\Theta}_i \|\Phi_{i21}\|^4 \\
&\quad - \frac{3\varepsilon_{i23}^2}{4} \bar{\zeta}_{i2} \tilde{\Theta}_i \|\Phi_{i22}\|^2 - \frac{3\varepsilon_{i22}^2}{4} \bar{\zeta}_{i2} - \frac{3\varepsilon_{i24}^2}{4} \bar{\zeta}_{i2} \\
&\quad - \frac{3}{4} \bar{\zeta}_{i2} - \xi_i q_i \eta_{i1} - \frac{3^3}{4} \xi_i^4 q_i^4 \bar{\zeta}_{i2}. \quad (26)
\end{aligned}$$

By substituting Eq. (26) to inequality (25), it obtains

$$\mathcal{L}V_{i2} \leq \bar{\zeta}_{i2}^3 \bar{\zeta}_{i3} - \sum_{j=1}^2 k_{ij} \bar{\zeta}_{ij}^4 - \bar{\zeta}_{i2}^4 + \frac{1}{\delta_i} \tilde{\Theta}_i (\Delta_{i2} - \dot{\Theta}_i) + \Upsilon_{i2}$$

where $\Delta_{i2} = \Delta_{i1} + \frac{3\varepsilon_{i21}^2}{4} \bar{\zeta}_{i2}^4 \|\Phi_{i21}\|^4 + \frac{3\varepsilon_{i23}^2}{4} \bar{\zeta}_{i2}^4 \|\Phi_{i22}\|^2$, and $\Upsilon_{i2} = \Upsilon_{i1} + \frac{1}{4\varepsilon_{i21}^4} + \frac{\varepsilon_{i21}^4}{4\varepsilon_{i22}^4} + \frac{3}{4\varepsilon_{i23}^2} + \frac{3\varepsilon_{i22}^2}{4\varepsilon_{i24}^2} + \frac{\lambda_{i2}^4}{4}$.

Step o ($2 < o < n_i$): Choose the Lyapunov function as

$$V_{io} = V_{i(o-1)} + \frac{1}{4} \bar{\zeta}_{io}^4$$

where $\bar{\zeta}_{io} = \zeta_{io} - \eta_{io}$. Similar to Eq. (23), to eliminate the filtering error $\alpha_{io}^* - \alpha_{io}$, the o -th compensation signal η_{io} is designed as

$$\dot{\eta}_{io} = - (k_{io} + 1) \eta_{io} + (\alpha_{io}^* - \alpha_{io}) - \eta_{i(o-1)} + \eta_{i(o+1)} - \lambda_{io} \text{sgn}(\eta_{io})$$

where k_{io} and λ_{io} are positive designed parameters.

The infinitesimal generator of V_{io} satisfies

$$\begin{aligned} \mathcal{L}V_{io} \leq & \bar{\zeta}_{io}^3 \left[\bar{\zeta}_{i(o+1)} + \alpha_{io} + f_{io} - \dot{\alpha}_{i(o-1)}^* + (k_{io} + 1) \eta_{io} \right. \\ & \left. + \eta_{i(o-1)} + \lambda_{io} \text{sgn}(\eta_{io}) \right] + \frac{3}{2} \bar{\zeta}_{io}^2 g_{io} g_{io}^T + \bar{\zeta}_{i(o-1)}^3 \bar{\zeta}_{io} \\ & - \sum_{j=1}^{o-1} k_{ij} \bar{\zeta}_{ij}^4 - \bar{\zeta}_{i(o-1)}^4 + \frac{1}{\delta_i} \bar{\Theta}_i \left[\Delta_{i(o-1)} - \dot{\Theta}_i \right] + \Upsilon_{i(o-1)} \end{aligned}$$

where f_{io} and $g_{io} g_{io}^T$ are unknown nonlinear functions. Similar to the relationships (19) and (20), we directly present the processing result as follows

$$\bar{\zeta}_{io}^3 f_{io} \leq \frac{3\varepsilon_{io1}^{\frac{4}{3}}}{4} \bar{\zeta}_{io}^4 \Theta_i \|\Phi_{io1}\|^{\frac{4}{3}} + \frac{1}{4\varepsilon_{io1}^4} + \frac{3\varepsilon_{io2}^{\frac{4}{3}}}{4} \bar{\zeta}_{io}^4 + \frac{\varepsilon_{io1}^{*4}}{4\varepsilon_{io2}^4}$$

where ε_{io1} and ε_{io2} are positive designed parameters. ε_{io1}^* is any given positive constant. Meanwhile, the following inequality can be obtained

$$\frac{3}{2} \bar{\zeta}_{io}^2 g_{io} g_{io}^T \leq \frac{3\varepsilon_{io3}^2}{4} \bar{\zeta}_{io}^4 \Theta_i \|\Phi_{io2}\|^2 + \frac{3}{4\varepsilon_{io3}^2} + \frac{3\varepsilon_{io4}^2}{4} \bar{\zeta}_{io}^4 + \frac{3\varepsilon_{io2}^{*2}}{4\varepsilon_{io4}^2}$$

where ε_{io3} and ε_{io4} are positive designed parameters, and ε_{io2}^* is any given positive constant. By using Lemma 6, we have

$$\begin{cases} \bar{\zeta}_{i(o-1)}^3 \bar{\zeta}_{io} \leq \bar{\zeta}_{i(o-1)}^4 + \frac{3^3}{4^4} \bar{\zeta}_{io}^4 \\ \bar{\zeta}_{io}^3 \lambda_{io} \text{sgn}(\eta_{io}) \leq \frac{3}{4} \bar{\zeta}_{io}^4 + \frac{\lambda_{io}^4}{4} \end{cases}$$

Based on the above inequalities, $\mathcal{L}V_{io}$ further satisfies the following inequality

$$\begin{aligned} \mathcal{L}V_{io} \leq & \bar{\zeta}_{io}^3 \left(\bar{\zeta}_{i(o+1)} + \alpha_{io} + \frac{3\varepsilon_{io1}^{\frac{4}{3}}}{4} \bar{\zeta}_{io} \Theta_i \|\Phi_{io1}\|^{\frac{4}{3}} + \frac{3\varepsilon_{io2}^{\frac{4}{3}}}{4} \bar{\zeta}_{io} \right. \\ & \left. + \frac{3\varepsilon_{io3}^2}{4} \bar{\zeta}_{io} \Theta_i \|\Phi_{io2}\|^2 + \frac{3\varepsilon_{io4}^2}{4} \bar{\zeta}_{io} - \dot{\alpha}_{i(o-1)}^* + \frac{3}{4} \bar{\zeta}_{io} \right. \\ & \left. + \eta_{i(o-1)} + (k_{io} + 1) \eta_{io} + \frac{3^3}{4^4} \bar{\zeta}_{io} \right) + \frac{1}{4\varepsilon_{io1}^4} \\ & + \frac{\varepsilon_{io1}^{*4}}{4\varepsilon_{io2}^4} + \frac{3}{4\varepsilon_{io3}^2} + \frac{3\varepsilon_{io2}^{*2}}{4\varepsilon_{io4}^2} + \frac{\lambda_{io}^4}{4} - \sum_{j=1}^{o-1} k_{ij} \bar{\zeta}_{ij}^4 \\ & + \frac{1}{\delta_i} \bar{\Theta}_i \left[\Delta_{i(o-1)} - \dot{\Theta}_i \right] + \Upsilon_{i(o-1)}. \end{aligned} \quad (27)$$

According to inequality (27), the virtual controller α_{io} can be constructed as

$$\begin{aligned} \alpha_{io} = & - (k_{io} + 1) \zeta_{io} + \dot{\alpha}_{i(o-1)}^* - \frac{3\varepsilon_{io1}^{\frac{4}{3}}}{4} \bar{\zeta}_{io} \bar{\Theta}_i \|\Phi_{io1}\|^{\frac{4}{3}} \\ & - \frac{3\varepsilon_{io3}^2}{4} \bar{\zeta}_{io} \bar{\Theta}_i \|\Phi_{io2}\|^2 - \frac{3\varepsilon_{io2}^{\frac{4}{3}}}{4} \bar{\zeta}_{io} - \frac{3\varepsilon_{io4}^2}{4} \bar{\zeta}_{io} \\ & - \frac{3}{4} \bar{\zeta}_{io} - \frac{3^3}{4^4} \bar{\zeta}_{io} - \eta_{i(o-1)}. \end{aligned} \quad (28)$$

By substituting Eq. (28) to inequality (27), it gets

$$\mathcal{L}V_{io} \leq \bar{\zeta}_{io}^3 \bar{\zeta}_{i(o+1)} - \sum_{j=1}^o k_{ij} \bar{\zeta}_{ij}^4 - \bar{\zeta}_{io}^4 + \frac{1}{\delta_i} \bar{\Theta}_i (\Delta_i - \dot{\Theta}_i) + \Upsilon_{io}$$

where $\Delta_{io} = \Delta_{i(o-1)} + \frac{3\varepsilon_{io1}^{\frac{4}{3}}}{4} \bar{\zeta}_{io}^4 \|\Phi_{io1}\|^{\frac{4}{3}} + \frac{3\varepsilon_{io2}^2}{4} \bar{\zeta}_{io}^4 \|\Phi_{io2}\|^2$, and $\Upsilon_{io} = \Upsilon_{i(o-1)} + \frac{1}{4\varepsilon_{io1}^4} + \frac{\varepsilon_{io1}^{*4}}{4\varepsilon_{io2}^4} + \frac{3}{4\varepsilon_{io3}^2} + \frac{3\varepsilon_{io2}^{*2}}{4\varepsilon_{io4}^4} + \frac{\lambda_{io}^4}{4}$.

Step n_i : In this section, the fault-tolerant controller u_{ih} will be constructed. For subsequent stability analysis of the controller, the compensation signal η_{in_i} is defined as

$$\dot{\eta}_{in_i} = - (k_{in_i} + 1) \eta_{in_i} - \eta_{i(n_i-1)} - \lambda_{in_i} \text{sgn}(\eta_{in_i})$$

where k_{in_i} and λ_{in_i} are positive designed parameters.

Based on Assumption 2, it is not difficult to conclude $\inf_{i \geq 0} \sum_{h=1}^M |l_{ih}| \rho_{ih} \geq \min\{|l_{i1}| \rho_{i1}, \dots, |l_{iM}| \rho_{iM}\} > 0$.

To construct subsequent Lyapunov function V_{in_i} , unknown constants ϱ_i and ϑ_i are defined as

$$\begin{aligned} \varrho_i &= \inf_{i \geq 0} \sum_{h=1}^M |l_{ih}| \rho_{ih}, \quad \varphi_i = \frac{1}{\varrho_i} \\ \vartheta_i &= \sup_{i \geq 0} \sum_{h=1}^M |l_{ih}| \nu_{ih}. \end{aligned}$$

The Lyapunov function is selected as

$$V_{in_i} = V_{i(n_i-1)} + \frac{1}{4} \bar{\zeta}_{in_i}^4 + \frac{\varrho_i}{2\Psi_i} \bar{\varphi}_i^2 + \frac{1}{2\Gamma_i} \bar{\vartheta}_i^2$$

where Ψ_i and Γ_i are positive design parameters, and $\bar{\zeta}_{in_i} = \zeta_{in_i} - \eta_{in_i}$ is a compensated error.

Similar to Eq. (24), the infinitesimal generator of V_{in_i} satisfies the following relationship

$$\begin{aligned} \mathcal{L}V_{in_i} \leq & \bar{\zeta}_{i(n_i-1)}^3 \bar{\zeta}_{in_i} - \sum_{j=1}^{n_i-1} k_{ij} \bar{\zeta}_{ij}^4 - \bar{\zeta}_{i(n_i-1)}^4 + \Upsilon_{i(n_i-1)} \\ & + \frac{1}{\delta_i} \bar{\Theta}_i (\Delta_{in_i} - \dot{\Theta}_i) + \frac{3}{2} \bar{\zeta}_{in_i}^2 g_{in_i} g_{in_i}^T \\ & + \bar{\zeta}_{in_i}^3 \left(\sum_{h=1}^M l_{ih} (\rho_{ih} u_{ih} + \nu_{ih}) + f_{in_i} - \dot{\alpha}_{i(n_i-1)}^* \right. \\ & \left. + (k_{in_i} + 1) \eta_{in_i} + \eta_{i(n_i-1)} + \lambda_{in_i} \text{sgn}(\eta_{in_i}) \right) \\ & - \frac{\varrho_i}{\Psi_i} \bar{\varphi}_i \dot{\bar{\varphi}}_i - \frac{1}{\Gamma_i} \bar{\vartheta}_i \dot{\bar{\vartheta}}_i \end{aligned} \quad (29)$$

where f_{in_i} and $g_{in_i} g_{in_i}^T$ are unknown functions. Similar to the relationships (19) and (20), one has

$$\bar{\zeta}_{in_i}^3 f_{in_i} \leq \frac{3\varepsilon_{in_i1}^{\frac{4}{3}}}{4} \bar{\zeta}_{in_i}^4 \Theta_i \|\Phi_{in_i1}\|^{\frac{4}{3}} + \frac{1}{4\varepsilon_{in_i1}^4} + \frac{3\varepsilon_{in_i2}^{\frac{4}{3}}}{4} \bar{\zeta}_{in_i}^4 + \frac{\varepsilon_{in_i1}^{*4}}{4\varepsilon_{in_i2}^4}$$

where ε_{in_i1} and ε_{in_i2} are positive designed parameters. $\varepsilon_{in_i1}^*$ is any given positive constant. At the same time, we have

$$\begin{aligned} \frac{3}{2} \bar{\zeta}_{in_i}^2 g_{in_i} g_{in_i}^T \leq & \frac{3\varepsilon_{in_i3}^2}{4} \bar{\zeta}_{in_i}^4 \Theta_i \|\Phi_{in_i1}\|^2 + \frac{3}{4\varepsilon_{in_i3}^2} \\ & + \frac{3\varepsilon_{in_i4}^2}{4} \bar{\zeta}_{in_i}^4 + \frac{3\varepsilon_{in_i2}^{*2}}{4\varepsilon_{in_i4}^2} \end{aligned}$$

where ε_{in_3} and ε_{in_4} are positive designed parameters. The scalar $\epsilon_{in_2}^*$ is a positive constant. By Lemma 6, one gets

$$\begin{cases} \bar{\zeta}_{i(n_i-1)}^3 \bar{\zeta}_{in_i} \leq \bar{\zeta}_{i(n_i-1)}^4 + \frac{3^3}{4^4} \bar{\zeta}_{in_i}^4 \\ \bar{\zeta}_{in_i}^3 \lambda_{in_i} \text{sgn}(\eta_{in_i}) \leq \bar{\zeta}_{in_i}^4 + \frac{3^3}{4^4} \lambda_{in_i}^4. \end{cases}$$

By substituting the above inequalities to (29), one has

$$\begin{aligned} \mathcal{L}V_{in_i} \leq & - \sum_{j=1}^{n_i-1} k_{ij} \bar{\zeta}_{ij}^4 + \frac{1}{\delta_i} \bar{\Theta}_i (\Delta_{i(n_i-1)} - \dot{\Theta}_i) + \Upsilon_{i(n_i-1)} \\ & + \bar{\zeta}_{in_i}^3 \left(\sum_{h=1}^M l_{ih} \rho_{ihl} u_{ih} + \sum_{h=1}^M l_{ih} \nu_{ihl} + \bar{u}_i - \bar{u}_i \right. \\ & + \frac{3\varepsilon_{in_1}^4}{4} \bar{\zeta}_{in_i} \bar{\Theta}_i \|\Phi_{in_1}\|^{\frac{4}{3}} + \frac{3\varepsilon_{in_3}^2}{4} \bar{\zeta}_{in_i} \bar{\Theta}_i \|\Phi_{in_2}\|^2 \\ & + \frac{3\varepsilon_{in_2}^4}{4} \bar{\zeta}_{in_i} + \frac{3\varepsilon_{in_4}^2}{4} \bar{\zeta}_{in_i} + \frac{3^3}{4^4} \bar{\zeta}_{in_i} + \bar{\zeta}_{in_i} - \dot{\alpha}_{i(n_i-1)}^* \\ & \left. + (k_{in_i} + 1) \eta_{in_i} + \eta_{i(n_i-1)} \right) - \frac{\varrho_i}{\Psi_i} \tilde{\varphi}_i \dot{\varphi}_i - \frac{1}{\Gamma_i} \tilde{\vartheta}_i \dot{\vartheta}_i \\ & + \frac{3^3}{4^4} \lambda_{in_i}^4 + \frac{1}{4\varepsilon_{in_1}^4} + \frac{\epsilon_{in_1}^4}{4\varepsilon_{in_2}^4} + \frac{3}{4\varepsilon_{in_3}^2} + \frac{3\varepsilon_{in_2}^2}{4\varepsilon_{in_4}^2} \end{aligned} \quad (30)$$

where \bar{u}_i is an intermediate control variable described by

$$\begin{aligned} \bar{u}_i = & (k_{in_i} + 1) \zeta_{in_i} + \frac{3\varepsilon_{in_1}^4}{4} \bar{\zeta}_{in_i} \bar{\Theta}_i \|\Phi_{in_1}\|^{\frac{4}{3}} + \frac{3\varepsilon_{in_2}^2}{4} \bar{\zeta}_{in_i} \\ & + \frac{3\varepsilon_{in_3}^2}{4} \bar{\zeta}_{in_i} \bar{\Theta}_i \|\Phi_{in_2}\|^2 + \frac{3\varepsilon_{in_4}^2}{4} \bar{\zeta}_{in_i} + \frac{3^3}{4^4} \bar{\zeta}_{in_i} \\ & - \dot{\alpha}_{i(n_i-1)}^* + \eta_{i(n_i-1)} + \hat{\vartheta}_i \tanh\left(\frac{\bar{\zeta}_{in_i}}{\epsilon_i}\right) \end{aligned} \quad (31)$$

and ϵ_i is a positive designed parameter. By substituting Eq. (31) to inequality (30), one gets

$$\begin{aligned} \mathcal{L}V_{in_i} \leq & - \sum_{j=1}^{n_i} k_{ij} \bar{\zeta}_{ij}^4 + \frac{1}{\delta_i} \bar{\Theta}_i (\Delta_{in_i} - \dot{\Theta}_i) + \Upsilon_{i(n_i-1)} \\ & + \bar{\zeta}_{in_i}^3 \sum_{h=1}^M l_{ih} \rho_{ihl} u_{ih} + \bar{\zeta}_{in_i}^3 \bar{u}_i + \frac{3^3}{4^4} \lambda_{in_i}^4 \\ & - \frac{\varrho_i}{\Psi_i} \tilde{\varphi}_i \dot{\varphi}_i - \frac{1}{\Gamma_i} \tilde{\vartheta}_i \left(\dot{\vartheta}_i - \Gamma_i \bar{\zeta}_{in_i}^3 \tanh\left(\frac{\bar{\zeta}_{in_i}}{\epsilon_i}\right) \right) \\ & + \vartheta_i \left(|\bar{\zeta}_{in_i}^3| - \bar{\zeta}_{in_i}^3 \tanh\left(\frac{\bar{\zeta}_{in_i}}{\epsilon_i}\right) \right) + \frac{1}{4\varepsilon_{in_1}^4} \\ & + \frac{\epsilon_{in_1}^4}{4\varepsilon_{in_2}^4} + \frac{3}{4\varepsilon_{in_3}^2} + \frac{3\varepsilon_{in_2}^2}{4\varepsilon_{in_4}^2}. \end{aligned} \quad (32)$$

The variable Δ_{in_i} satisfies

$$\Delta_{in_i} = \Delta_{i(n_i-1)} + \frac{3\delta_i \varepsilon_{in_1}^4}{4} \bar{\zeta}_{in_i}^4 \|\Phi_{in_1}\|^{\frac{4}{3}} + \frac{3\delta_i \varepsilon_{in_3}^2}{4} \bar{\zeta}_{in_i}^4 \|\Phi_{in_2}\|^2.$$

The fault-tolerant controller u_{ih} is designed as

$$u_{ih} = \text{sgn}(l_{ih}) \bar{\alpha}_{in_i}, \quad \bar{\alpha}_{in_i} = - \frac{\bar{\zeta}_{in_i}^3 \hat{\varphi}_i^2 \bar{u}_i^2}{\sqrt{\bar{\zeta}_{in_i}^6 \hat{\varphi}_i^2 \bar{u}_i^2 + \varepsilon_{in_5}^2}} \quad (33)$$

where ε_{in_5} is a positive designed parameter. The adaptive laws are constructed as

$$\begin{cases} \dot{\Theta}_i = \Delta_{in_i} - \bar{\delta}_i \bar{\Theta}_i \\ \dot{\hat{\vartheta}}_i = \Gamma_i \bar{\zeta}_{in_i}^3 \tanh\left(\frac{\bar{\zeta}_{in_i}}{\epsilon_i}\right) - \bar{\Gamma}_i \hat{\vartheta}_i \\ \dot{\hat{\varphi}}_i = \Psi_i \bar{\zeta}_{in_i}^3 \bar{u}_i - \bar{\Psi}_i \hat{\varphi}_i \end{cases} \quad (34)$$

where $\bar{\delta}_i$, $\bar{\Gamma}_i$ and $\bar{\Psi}_i$ are positive designed parameters. By Lemma 7, it is not hard to derive

$$\begin{aligned} \bar{\zeta}_{in_i}^3 \sum_{h=1}^M l_{ih} \rho_{ihl} u_{ih} &= - \sum_{h=1}^M |l_{ih}| \rho_{ihl} \frac{\bar{\zeta}_{in_i}^6 \hat{\varphi}_i^2 \bar{u}_i^2}{\sqrt{\bar{\zeta}_{in_i}^6 \hat{\varphi}_i^2 \bar{u}_i^2 + \varepsilon_{in_5}^2}} \\ &\leq - \frac{\varrho_i \bar{\zeta}_{in_i}^6 \hat{\varphi}_i^2 \bar{u}_i^2}{\sqrt{\bar{\zeta}_{in_i}^6 \hat{\varphi}_i^2 \bar{u}_i^2 + \varepsilon_{in_5}^2}} \\ &\leq \varrho_i \varepsilon_{in_5} - \varrho_i \bar{\zeta}_{in_i}^3 \hat{\varphi}_i \bar{u}_i. \end{aligned} \quad (35)$$

Based on the fact that $0 \leq |\aleph| - \aleph \tanh\left(\frac{\aleph}{\bar{\varrho}}\right) \leq 0.2785 \bar{\varrho}$ and relationships (33)-(35), inequality (32) can be rewritten as

$$\begin{aligned} \mathcal{L}V_{in_i} \leq & - \sum_{j=1}^{n_i} k_{ij} \bar{\zeta}_{ij}^4 + \frac{\bar{\delta}_i}{\delta_i} \bar{\Theta}_i \dot{\Theta}_i + \frac{\varrho_i \bar{\Psi}_i}{\Psi_i} \tilde{\varphi}_i \dot{\varphi}_i + \frac{\bar{\Gamma}_i}{\Gamma_i} \tilde{\vartheta}_i \dot{\vartheta}_i \\ & + \Upsilon_{i(n_i-1)} + \frac{3^3}{4^4} \lambda_{in_i}^4 + \frac{1}{4\varepsilon_{in_1}^4} + \frac{\epsilon_{in_1}^4}{4\varepsilon_{in_2}^4} + \frac{3}{4\varepsilon_{in_3}^2} \\ & + \frac{3\varepsilon_{in_2}^2}{4\varepsilon_{in_4}^2} + 0.2785 \vartheta_i \bar{\varrho}_i + \varrho_i \varepsilon_{in_5} \end{aligned} \quad (36)$$

where $\bar{\varrho}$ is a positive constant, and the variable $\aleph \in R$. By Lemma 6, it is not difficult to get

$$\begin{cases} \frac{\bar{\Gamma}_i}{\Gamma_i} \tilde{\vartheta}_i \dot{\vartheta}_i \leq - \frac{\bar{\Gamma}_i}{2\Gamma_i} \tilde{\vartheta}_i^2 + \frac{\bar{\Gamma}_i}{2\Gamma_i} \vartheta_i^2 \\ \frac{\bar{\delta}_i}{\delta_i} \bar{\Theta}_i \dot{\Theta}_i \leq - \frac{\bar{\delta}_i}{2\delta_i} \bar{\Theta}_i^2 + \frac{\bar{\delta}_i}{2\delta_i} \Theta_i^2 \\ \frac{\bar{\Psi}_i}{\Psi_i} \tilde{\varphi}_i \dot{\varphi}_i \leq - \frac{\varrho_i \bar{\Psi}_i}{2\Psi_i} \tilde{\varphi}_i^2 + \frac{\varrho_i \bar{\Psi}_i}{2\Psi_i} \varphi_i^2. \end{cases}$$

Then inequality (36) can be rewritten as

$$\mathcal{L}V_{in_i} \leq - \sum_{j=1}^{n_i} k_{ij} \bar{\zeta}_{ij}^4 - \frac{\bar{\delta}_i}{2\delta_i} \bar{\Theta}_i^2 - \frac{\varrho_i \bar{\Psi}_i}{2\Psi_i} \tilde{\varphi}_i^2 - \frac{\bar{\Gamma}_i}{2\Gamma_i} \tilde{\vartheta}_i^2 + \Upsilon_{in_i}$$

where $\Upsilon_{in_i} = \Upsilon_{i(n_i-1)} + \frac{3^3}{4^4} \lambda_{in_i}^4 + \frac{1}{4\varepsilon_{in_1}^4} + \frac{\epsilon_{in_1}^4}{4\varepsilon_{in_2}^4} + \frac{3}{4\varepsilon_{in_3}^2} + \frac{3\varepsilon_{in_2}^2}{4\varepsilon_{in_4}^2} + 0.2785 \vartheta_i \bar{\varrho}_i + \varrho_i \varepsilon_{in_5} + \frac{\bar{\Gamma}_i}{2\Gamma_i} \vartheta_i^2 + \frac{\bar{\delta}_i}{2\delta_i} \Theta_i^2 + \frac{\varrho_i \bar{\Psi}_i}{2\Psi_i} \varphi_i^2$.

Remark 3: In the design of the fault-tolerant controller, we adopt two FLSs to deal with unknown nonlinear dynamics in drift and diffusion terms, respectively. Generally speaking, the number of adaptive laws increases as the order of the agent increases, which will lead to the over-parameterization problem. Inspired by [42], a less parameter estimation approach is adopted, which makes the number of adaptive laws independent of the order of the system. Therefore, this approach avoids the problem of over-parameterization and reduces the computational burden in results [43] and [44].

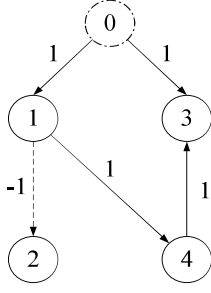


Fig. 1. The communication topology in *Numerical Example*.

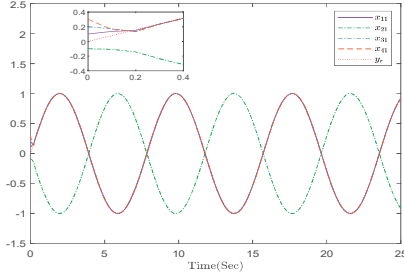


Fig. 2. Output trajectories of agents in *Numerical Example*.

V. STABILITY ANALYSIS

Theorem 1: For stochastic nonlinear MASs (9) with virtual controllers (22) and (28), the fault-tolerant controller (33) and adaptive laws (34), if *Assumptions* 1-3 and the condition $|z_{i1}(0)| \in (0, \sigma(0))$ are satisfied, then *control objectives* (a) and (b) can be achieved.

Proof: Firstly, to prove that the compensation signal η_{ij} is bounded, the following Lyapunov function is considered

$$V_{i\eta} = \sum_{j=1}^{n_i} \frac{\eta_{ij}^2}{2}.$$

Then, it obtains

$$\begin{aligned} \dot{V}_{i\eta} = & -(k_{i1} + 1)\eta_{i1}^2 + \xi_i q_i (\alpha_{i1}^* - \alpha_{i1}) \eta_{i1} \\ & + \xi_i q_i \eta_{i1} \eta_{i2} - \lambda_{i1} \xi_i q_i |\eta_{i1}| \\ & - (k_{i2} + 1)\eta_{i2}^2 + (\alpha_{i2}^* - \alpha_{i2}) \eta_{i2} - \xi_i q_i \eta_{i1} \eta_{i2} \\ & + \eta_{i2} \eta_{i3} - \lambda_{i2} |\eta_{i2}| \\ & \dots \\ & - (k_{in_i} + 1)\eta_{in_i}^2 - \eta_{i(n_i-1)} \eta_{in_i} - \lambda_{in_i} |\eta_{in_i}|. \end{aligned} \quad (37)$$

According to the results in [45], the filter error satisfies the condition that $\|\alpha_{ij}^* - \alpha_{ij}\| \leq \sigma_{ij}$ in a finite time with a known constant σ_{ij} . Then, Eq. (37) can be rewritten

$$\dot{V}_{i\eta} \leq - \sum_{j=1}^{n_i} (k_{ij} + 1) \eta_{ij}^2 + \sum_{j=1}^{n_i} \bar{l}_j \sigma_{ij} |\eta_{ij}| - \sum_{j=1}^{n_i} \bar{l}_j \lambda_{ij} |\eta_{ij}|$$

where $\bar{l}_1 = \xi_i q_i$, and $\bar{l}_j = 1$ with $j = 2, 3, \dots, n_i$. By selecting appropriate parameters so that σ_{ij} and λ_{ij} satisfy the condition that $\sigma_{ij} < \lambda_{ij}$, it gets

$$\dot{V}_{i\eta} \leq - \sum_{j=1}^{n_i} (k_{ij} + 1) \eta_{ij}^2$$

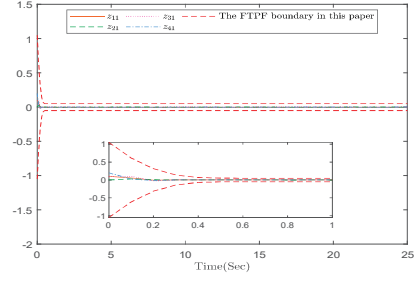


Fig. 3. Bipartite consensus errors z_{i1} under the constraint of the FTPF in this paper.

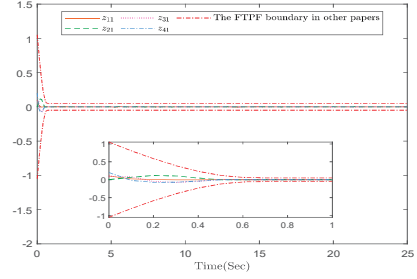


Fig. 4. Bipartite consensus errors z_{i1} under the constraint of the FTPF in [25]–[28].

which indicates that the compensation signal η_{ij} can exponentially converge to 0.

Construct the following Lyapunov function

$$V = \sum_{i=1}^N V_{in_i}.$$

Then, one obtains

$$\begin{aligned} \mathcal{L}V \leq & \sum_{i=1}^N \left(- \sum_{j=1}^{n_i} k_{ij} \bar{\zeta}_{ij}^4 - \frac{\bar{\delta}_i}{2\delta_i} \bar{\Theta}_i^2 - \frac{\bar{\rho}_i \bar{\Psi}_i}{2\bar{\Psi}_i} \bar{\varphi}_i^2 - \frac{\bar{\Gamma}_i}{2\bar{\Gamma}_i} \bar{\vartheta}_i^2 + \Upsilon_{in_i} \right) \\ \leq & -cV + b \end{aligned} \quad (38)$$

where $c = \min\{4k_{ij}, \bar{\delta}_i, \bar{\Psi}_i, \bar{\Gamma}_i\}$, $b = \sum_{i=1}^N \Upsilon_{in_i}$. From Eq. (38) and Lemma 3, it gets

$$E(V) \leq V(0)e^{-ct} + \frac{b}{c}. \quad (39)$$

According to the definition of Lyapunov function V , inequality (39) indicates that signals $\bar{\zeta}_{ij}$, $\bar{\Theta}_i$, $\bar{\varphi}_i$ and $\bar{\vartheta}_i$ are all SGUUB in probability. Based on the convergence of compensation signal η_{ij} and the relationship $\zeta_{ij} = \bar{\zeta}_{ij} + \eta_{ij}$, it can be obtained that the signal ζ_{ij} is also SGUUB in probability. Furthermore, by considering the error transformation mechanism (12), the coordinate transformations (16), virtual control laws (22) and (28), and the fault-tolerant controller (33), we can get that all signals of agents are SGUUB in probability. The *control objective* (a) is achieved.

In addition, based on Eq. (12) and the fourth property of FTPF, it follows that

$$z_{i1} = \sigma_\infty \mu(e_{i1}^*), \quad \forall t \geq T_s$$

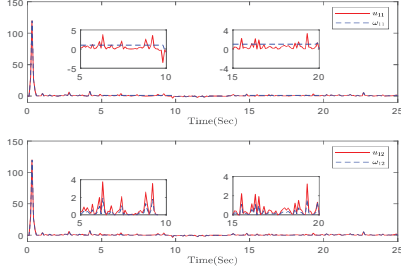


Fig. 5. The curves of actuator inputs and outputs of the first follower.

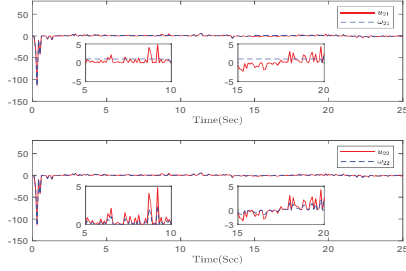


Fig. 6. The curves of actuator inputs and outputs of the second follower.

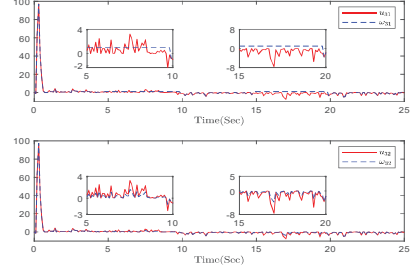


Fig. 7. The curves of actuator inputs and outputs of the third follower.

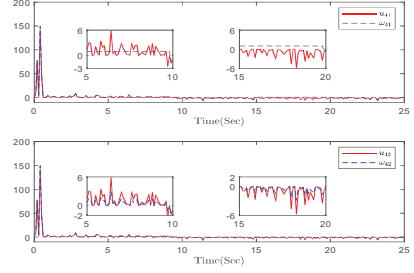


Fig. 8. The curves of actuator inputs and outputs of the fourth follower.

which indicates that the relationship $|z_{i1}| < \sigma_\infty$ holds. Then, for $\forall t \geq T_s$, we can further yield $E(\|z_{i1}\|) < \sigma_\infty$, which implies the *control objective* (b) is satisfied.

Moreover, define bipartite tracking errors $\tilde{e}_i = y_i - \mathfrak{F}_i y_r$ with $i = 1, 2, \dots, N$, and vectors $\tilde{e} = [\tilde{e}_1, \dots, \tilde{e}_N]^T$ and $z = [z_{11}, \dots, z_{N1}]^T$. Based on Lemma 1 and the fact that $z = (L_{\mathcal{G}} + B_{\mathcal{G}})\tilde{e}$, we have

$$\|\tilde{e}\| \leq \frac{\|z\|}{\hbar(L_{\mathcal{G}} + B_{\mathcal{G}})} \quad (40)$$

where $\hbar(L_{\mathcal{G}} + B_{\mathcal{G}})$ represents the minimum singular value of the matrix $(L_{\mathcal{G}} + B_{\mathcal{G}})$. Based on inequality (40) and the fact $|z_{i1}| < \sigma_\infty$, the following relationship holds

$$E(\|\tilde{e}\|) \leq \frac{E(\|z\|)}{\hbar(L_{\mathcal{G}} + B_{\mathcal{G}})} < \frac{\sigma_\infty \sqrt{N}}{\hbar(L_{\mathcal{G}} + B_{\mathcal{G}})}, \quad \forall t \geq T_s. \quad (41)$$

Due to the fact that σ_∞ can be arbitrarily small, inequality (41) indicates that the tracking error can also satisfy the arbitrary tracking precision with probability in the predefined settling time. The proof is completed. ■

VI. SIMULATION RESULTS

In this section, to verify its effectiveness, the proposed control scheme is applied to BCT tasks of second-order stochastic MASs and a group of vehicles, respectively.

Numerical Example: Consider MASs consisting of four followers (agents 1-4) and a leader (agent 0). The communication topology of MASs is denoted as Fig. 1. Based on Fig. 1, we

can obtain that $\hbar(L_{\mathcal{G}} + B_{\mathcal{G}}) = 1$. Let $y_r = \frac{30}{9} \sin(\frac{4t}{5})$ denote the leader signal. The i -th follower is modeled as

$$\begin{cases} dx_{i1} = (x_{i2} + 0.2x_{i1})dt + 0.2 \sin(6x_{i1})d\varpi \\ dx_{i2} = \left(\sum_{h=1}^2 l_{ih} \omega_{ih} + 0.2x_{i1}x_{i2} \right)dt + 0.2 \sin(6x_{i1}x_{i2})d\varpi \\ y_i = x_{i1}, \quad i = 1, 2, 3, 4. \end{cases}$$

The i -th follower suffers from the following actuator faults

$$\begin{cases} \omega_{i1}(t) = \nu_{i1\iota}, \quad t \in [5\iota, 5(\iota+1)) \\ \omega_{i2}(t) = \rho_{i2\iota} u_{i2}(t), \quad \iota = 1, 3, \dots \end{cases} \quad (42)$$

where $\nu_{i1\iota} = 1$ and $\rho_{i2\iota} = 0.5$. Eq. (42) indicates that the first actuator operates in TLOE every 5 seconds, and the second actuator operates in PLOE every 5 seconds.

The designed parameters of $\sigma(t)$ are selected as $\sigma_0 = 1.05$, $\sigma_\infty = 0.05$, $\varsigma = 4$ and $T_s = 0.8$. The first fuzzy membership functions are chosen as $\phi_{f_i}^\iota(x_i) = e^{-0.5(x_i - \check{x}_\iota)^2}$ with $\iota = 1, 2, \dots, 7$, where $\check{x}_1 = -1.5$, $\check{x}_2 = -1$, $\check{x}_3 = -0.5$, $\check{x}_4 = 0$, $\check{x}_5 = 0.5$, $\check{x}_6 = 1$, $\check{x}_7 = 1.5$. The second fuzzy membership functions are chosen as $\phi_{g_i}^\iota(x_i) = e^{-0.5(x_i - \check{\bar{x}}_\iota)^2}$ with $\iota = 1, 2, \dots, 7$, where $\check{\bar{x}}_1 = -2$, $\check{\bar{x}}_2 = -1.5$, $\check{\bar{x}}_3 = -0.5$, $\check{\bar{x}}_4 = 0$, $\check{\bar{x}}_5 = 0.5$, $\check{\bar{x}}_6 = 1.5$, $\check{\bar{x}}_7 = 2$. The initial states are set as $x_{11}(0) = 0.1$, $x_{21}(0) = -0.1$, $x_{31}(0) = 0.2$, $x_{41}(0) = 0.3$ and $x_{i2}(0) = 0$, $\hat{\Theta}_i(0) = 1$, $\hat{\vartheta}_i(0) = 1$ and $\hat{\varphi}_i(0) = 1$. The designed parameters of the controller are set as $k_{11} = k_{21} = k_{12} = k_{22} = 4$, $k_{31} = k_{41} = k_{32} = k_{42} = 12$, $l_{i1} = 1$, $l_{i2} = 2$, $\varepsilon_{i11} = \varepsilon_{i21} = 0.5$, $\varepsilon_{i12} = \varepsilon_{i22} = 0.1$, $\varepsilon_{i13} = \varepsilon_{i23} = 0.5$, $\varepsilon_{i14} = \varepsilon_{i24} = 0.1$, $\tau_i = 0.0125$, $\lambda_{i1} = \lambda_{i2} = 0.01$, $\epsilon_i = 0.1$, $\varepsilon_{i25} = 0.1$, $\delta_i = 4$, $\bar{\delta}_i = 0.5$, $\Gamma_i = 4$, $\bar{\Gamma}_i = 0.4$, $\Psi_i = 5$, $\bar{\Psi}_i = 0.2$.

The simulation results of the numerical example are presented in Figs. 2-8. Based on Lemma 2 and Fig. 1, we can obtain

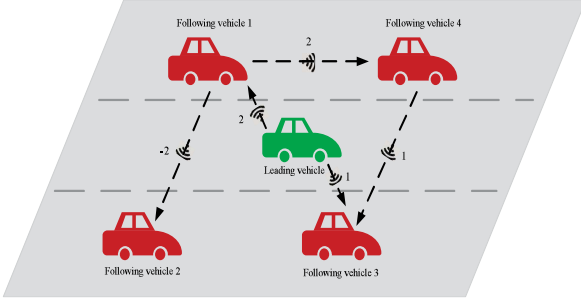
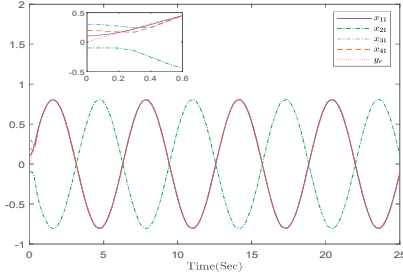


Fig. 9. Communication relationships among vehicles.

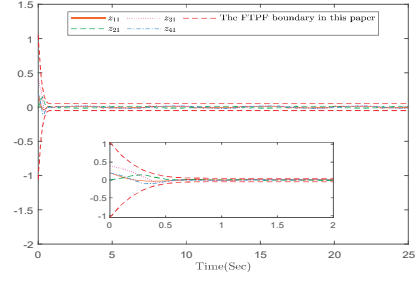
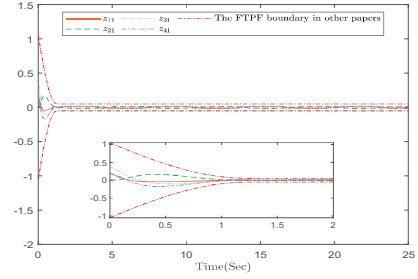
Fig. 10. Output trajectories of agents in *Practical Example*.

the bipartition of nodes $\mathbb{V}_1 = \{1, 3, 4\}$ and $\mathbb{V}_2 = \{2\}$, which means that agents 1, 3, 4 can track the leader signal and agent 2 can track the leader signal in an antisymmetric direction. The results in Fig. 2 verify this inference. Subsequently, in Fig. 3, we give curves for the bipartite consensus errors z_{i1} under the constraint of the FTPF in this paper. From Fig. 3, it can be concluded that $E(\|z_{i1}\|) < 0.05$ ($\forall t \geq 0.8$). Based on inequality (41), we can further obtain that $E(\|\dot{e}\|) < 0.1$ ($\forall t \geq 0.8$). Fig. 4 shows curves for the bipartite consensus errors z_{i1} under the constraint of the FTPF in [25]–[28]. By comparing Fig. 3 and Fig. 4, we can see that the FTPF in this paper improves the transient performance of MASs under the same conditions. Finally, Figs. 5–8 show the curves for the actuator inputs and outputs, and it can be seen that the first and second actuators suffer TLOE and PLOE every 5 seconds, respectively. From the above simulation results, it can be concluded that agents suffering from stochastic disturbances and actuator faults can still complete robust precision BCT tasks in a predefined settling time.

Practical Example: In this example, a group of vehicles [46] travelling on a firm horizontal surface are studied to further illustrate the effectiveness of the proposed control scheme. The communication relationships among vehicles are described in Fig. 9. Based on Fig. 9, we can calculate that $\bar{h}(L_g + B_g) = 2$. Suppose that the trajectory of the leading vehicle is $y_r = 0.8 \sin(t)$. The i -th following vehicle is modeled as

$$m_i \ddot{q}_i + \kappa_i m_i g + \varpi_i \dot{q}_i = \sum_{h=1}^2 \omega_{ih}, \quad i = 1, 2, 3, 4, \quad (43)$$

where \dot{q}_i and \ddot{q}_i represent the velocity and acceleration of the following vehicle, respectively. m_i denotes the mass of

Fig. 11. Bipartite consensus errors z_{i1} under the constraint of the FTPF in this paper.Fig. 12. Bipartite consensus errors z_{i1} under the constraint of the FTPF in [25]–[28].

the vehicle. κ_i is the kinetic friction coefficient. g is the acceleration of gravity. $\varpi_i \dot{q}_i$ is a viscous friction with an unknown constant ϖ . Assume that $\varpi_i = \hat{\varpi}_i + \mathcal{S}_i W_t$, where $\hat{\varpi}_i$ and \mathcal{S}_i are constants, and W_t is a standard white noise process. Define state variables $x_{i1} = q_i$, $x_{i2} = \dot{q}_i$, then Eq. (43) can be rewritten as

$$\begin{cases} dx_{i1} = x_{i2} dt \\ dx_{i2} = \left(\sum_{h=1}^2 \frac{1}{m_i} \omega_{ih} - \frac{\hat{\varpi}_i}{m_i} x_{i2} - \kappa_i g \right) dt + \frac{\mathcal{S}_i}{m_i} d\varpi \\ y_i = x_{i1} \end{cases}$$

where $m_i = 0.5$ kg, $g = 10$ m/s², $\kappa_i = 0.02$, $\hat{\varpi}_i = 0.5$, $\mathcal{S}_i = 0.1$, and ω_{ih} ($h = 1, 2$) are the same as Eq. (42).

The designed parameters of $\sigma(t)$ are selected as $\sigma_0 = 1.05$, $\sigma_\infty = 0.05$, $\varsigma = 6$ and $T_s = 1.5$. Based on inequality (41), with the help of the FTPF, the inequality $E(\|\dot{e}\|) < 0.05$ ($\forall t \geq 1.5$) holds, which indicates that the tracking precision of vehicles is set as ± 0.05 meter.

The fuzzy membership functions are the same as the numerical example. The initial states of vehicles are set as $x_{11}(0) = 0.1$, $x_{21}(0) = -0.1$, $x_{31}(0) = 0.3$, $x_{41}(0) = 0.2$ and $x_{i2}(0) = 0$. The initial values of adaptive laws are chosen as $\hat{\theta}_i(0) = 1$, $\hat{\vartheta}_i(0) = 1$ and $\hat{\varphi}_i(0) = 1$. The designed parameters are set as $k_{i1} = k_{i2} = 5$, $\varepsilon_{i11} = \varepsilon_{i21} = 0.5$, $\varepsilon_{i12} = \varepsilon_{i22} = 0.1$, $\varepsilon_{i13} = \varepsilon_{i23} = 0.5$, $\varepsilon_{i14} = \varepsilon_{i24} = 0.1$, $\tau_i = 0.014$, $\lambda_{i1} = \lambda_{i2} = 0.01$, $\epsilon_i = 0.2$, $\varepsilon_{i25} = 0.2$, $\delta_i = 1$, $\bar{\delta}_i = 0.4$, $\Gamma_i = 1$, $\bar{\Gamma}_i = 0.4$, $\Psi_i = 1$, $\bar{\Psi}_i = 0.8$.

The simulation results of the practical example are presented in Figs. 10–16. The bipartite tracking trajectories of vehicles are shown in Fig. 10. Under the constraint of the FTPF in this

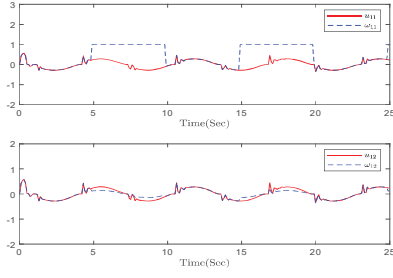


Fig. 13. The curves of actuator inputs and outputs of the first follower.

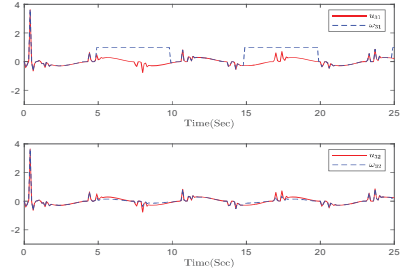


Fig. 15. The curves of actuator inputs and outputs of the third follower.

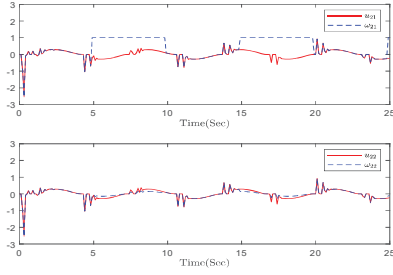


Fig. 14. The curves of actuator inputs and outputs of the second follower.

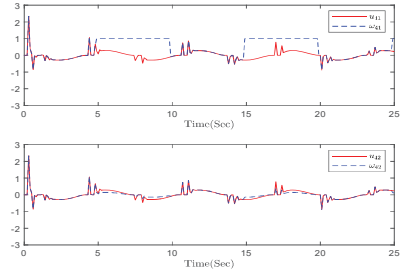


Fig. 16. The curves of actuator inputs and outputs of the fourth follower.

paper, bipartite consensus errors z_{i1} are presented in Fig. 11. Fig. 12 shows curves for bipartite consensus errors z_{i1} under the constraint of the FTPF in [25]–[28]. From Fig. 11 and Fig. 12, it can be concluded that $E(\|z_{i1}\|) < 0.05$ ($\forall t \geq 1.5$). Based on inequality (41), we can further obtain that $E(\|\dot{e}\|) < 0.05$ ($\forall t \geq 1.5$). By comparing Fig. 11 and Fig. 12, it is not hard to conclude that the FTPF in this paper improves the transient performance of vehicles systems under identical conditions. Finally, Figs. 13–16 show the curves of the actuator inputs and outputs, and it can be seen that the first and second actuators suffer TLOE and PLOE every 5 seconds, respectively. Based on Figs. 10–16, we can conclude that all vehicles subject to stochastic disturbances and actuator faults achieve finite-time robust precision BCT tasks.

VII. CONCLUSIONS

The presented paper has investigated finite-time robust precision BCT tasks for stochastic nonlinear MASs with actuator faults. An optimization-based FTPF has been proposed to improve the transient performance of MASs. Based on the FTPF, a fuzzy fault-tolerant distributed cooperative control scheme has been developed to ensure that all agents with various uncertainties complete robust precision BCT tasks in the predefined settling time. In addition, the less parameter estimation approach has been employed to avoid the over-parameterization problem in the controller design. Finally, the effectiveness of the proposed scheme has been verified in simulations, and the anticipated performance has been achieved in BCT tasks for a group of vehicles suffering from various uncertainties. For further extensions, we will continue to investigate how to achieve robust precision BCT tasks for MASs with unmeasurable states.

REFERENCES

- [1] M. E. Valcher and I. Zorzan, “On the consensus of homogeneous multi-agent systems with arbitrarily switching topology,” *Automatica*, vol. 84, pp. 79–85, 2017.
- [2] C. Ong and B. Hou, “Consensus of heterogeneous multi-agent system with input constraints,” *Automatica*, vol. 134, p. 109895, 2021.
- [3] H. Li, Y. Wu, M. Chen, and R. Lu, “Adaptive multigradient recursive reinforcement learning event-triggered tracking control for multiagent systems,” *IEEE Transactions on Neural Networks and Learning Systems*, DOI: 10.1109/TNNLS.2021.3090570, 2021.
- [4] S. J. Yoo, “Distributed consensus tracking for multiple uncertain nonlinear strict-feedback systems under a directed graph,” *IEEE Transactions on Neural Networks and Learning Systems*, vol. 24, no. 4, pp. 666–672, 2013.
- [5] G. Wen, H. Wang, X. Yu, and W. Yu, “Bipartite tracking consensus of linear multi-agent systems with a dynamic leader,” *IEEE Transactions on Circuits and Systems II: Express Briefs*, vol. 65, no. 9, pp. 1204–1208, 2018.
- [6] B. Ning, Q. Han, and Z. Zuo, “Bipartite consensus tracking for second-order multiagent systems: A time-varying function-based preset-time approach,” *IEEE Transactions on Automatic Control*, vol. 66, no. 6, pp. 2739–2745, 2021.
- [7] J. Shao, W. Zheng, L. Shi, and Y. Cheng, “Bipartite tracking consensus of generic linear agents with discrete-time dynamics over cooperation-competition networks,” *IEEE Transactions on Cybernetics*, vol. 51, no. 11, pp. 5225–5235, 2021.
- [8] X. Chen, L. Zhao, and J. Yu, “Adaptive neural finite-time bipartite consensus tracking of nonstrict feedback nonlinear competition multi-agent systems with input saturation,” *Neurocomputing*, vol. 397, pp. 168–178, 2020.
- [9] L. Zhao, Y. Jia, and J. Yu, “Adaptive finite-time bipartite consensus for second-order multi-agent systems with antagonistic interactions,” *Systems & Control Letters*, vol. 102, pp. 22–31, 2017.
- [10] Y. Wu, Y. Pan, M. Chen, and H. Li, “Quantized adaptive finite-time bipartite NN tracking control for stochastic multiagent systems,” *IEEE Transactions on Cybernetics*, vol. 51, no. 6, pp. 2870–2881, 2021.
- [11] H. Liang, X. Guo, Y. Pan, and T. Huang, “Event-triggered fuzzy bipartite tracking control for network systems based on distributed reduced-order observers,” *IEEE Transactions on Fuzzy Systems*, vol. 29, no. 6, pp. 1601–1614, 2021.
- [12] G. Liu, Q. Sun, H. Liang, and Z. Liu, “Antagonistic interactions-based adaptive event-triggered bipartite consensus quantized con-

- trol for stochastic multiagent systems,” *IEEE Systems Journal*, DOI: 10.1109/JSYST.2021.3116035, 2021.
- [13] T. Li, W. Bai, Q. Liu, Y. Long, and C. L. P. Chen, “Distributed fault-tolerant containment control protocols for the discrete-time multiagent systems via reinforcement learning method,” *IEEE Transactions on Neural Networks and Learning Systems*, DOI: 10.1109/TNNLS.2021.3121403, 2021.
 - [14] Y. Li, X. Shao, and S. Tong, “Adaptive fuzzy prescribed performance control of nontriangular structure nonlinear systems,” *IEEE Transactions on Fuzzy Systems*, vol. 28, no. 10, pp. 2416–2426, 2020.
 - [15] J. Zhang and G. Yang, “Fuzzy adaptive output feedback control of uncertain nonlinear systems with prescribed performance,” *IEEE Transactions on Cybernetics*, vol. 48, no. 5, pp. 1342–1354, 2018.
 - [16] S. He, M. Wang, S. Dai, and F. Luo, “Leader–follower formation control of USVs with prescribed performance and collision avoidance,” *IEEE Transactions on Industrial Informatics*, vol. 15, no. 1, pp. 572–581, 2019.
 - [17] S. Dai, S. He, M. Wang, and C. Yuan, “Adaptive neural control of underactuated surface vessels with prescribed performance guarantees,” *IEEE Transactions on Neural Networks and Learning Systems*, vol. 30, no. 12, pp. 3686–3698, 2019.
 - [18] J. Qiu, K. Sun, T. Wang, and H. Gao, “Observer-based fuzzy adaptive event-triggered control for pure-feedback nonlinear systems with prescribed performance,” *IEEE Transactions on Fuzzy Systems*, vol. 27, no. 11, pp. 2152–2162, 2019.
 - [19] J. Zhang and G. Yang, “Prescribed performance fault-tolerant control of uncertain nonlinear systems with unknown control directions,” *IEEE Transactions on Automatic Control*, vol. 62, no. 12, pp. 6529–6535, 2017.
 - [20] Y. Li and S. Tong, “Adaptive fuzzy control with prescribed performance for block-triangular-structured nonlinear systems,” *IEEE Transactions on Fuzzy Systems*, vol. 26, no. 3, pp. 1153–1163, 2018.
 - [21] D. Zhang, Z. Ye, G. Feng, and H. Li, “Intelligent event-based fuzzy dynamic positioning control of nonlinear unmanned marine vehicles under DoS attack,” *IEEE Transactions on Cybernetics*, DOI: 10.1109/TCYB.2021.3128170, 2021.
 - [22] W. He, X. Mu, L. Zhang, and Y. Zou, “Modeling and trajectory tracking control for flapping-wing micro aerial vehicles,” *IEEE/CAA Journal of Automatica Sinica*, vol. 8, no. 1, pp. 148–156, 2021.
 - [23] X. Shanguan, Y. He, C. Zhang, L. Jin, W. Yao, L. Jiang, and M. Wu, “Control performance standards-oriented event-triggered load frequency control for power systems under limited communication bandwidth,” *IEEE Transactions on Control Systems Technology*, vol. 30, no. 2, pp. 860–868, 2022.
 - [24] H. Liang, Z. Du, T. Huang, and Y. Pan, “Neuroadaptive performance guaranteed control for multiagent systems with power integrators and unknown measurement sensitivity,” *IEEE Transactions on Neural Networks and Learning Systems*, DOI: 10.1109/TNNLS.2022.3160532, 2022.
 - [25] Y. Liu, X. Liu, and Y. Jing, “Adaptive neural networks finite-time tracking control for non-strict feedback systems via prescribed performance,” *Information Sciences*, vol. 468, pp. 29–46, 2018.
 - [26] H. Wang, W. Bai, X. Zhao, and P. X. Liu, “Finite-time-prescribed performance-based adaptive fuzzy control for strict-feedback nonlinear systems with dynamic uncertainty and actuator faults,” *IEEE Transactions on Cybernetics*, DOI: 10.1109/TCYB.2020.3046316, 2021.
 - [27] Y. Liu, X. Liu, and Y. Jing, “Adaptive fuzzy finite-time stability of uncertain nonlinear systems based on prescribed performance,” *Fuzzy Sets and Systems*, vol. 374, pp. 23–39, 2019.
 - [28] Y. Liu, H. Li, Z. Zuo, X. Li, and R. Lu, “An overview of finite/fixed-time control and its application in engineering systems,” *IEEE/CAA Journal of Automatica Sinica*, DOI: 10.1109/JAS.2022.105413, 2022.
 - [29] S. Sui, C. L. P. Chen, and S. Tong, “A novel adaptive NN prescribed performance control for stochastic nonlinear systems,” *IEEE Transactions on Neural Networks and Learning Systems*, vol. 32, no. 7, pp. 3196–3205, 2021.
 - [30] Y. Liu, X. Liu, Y. Jing, and Z. Zhang, “A novel finite-time adaptive fuzzy tracking control scheme for nonstrict feedback systems,” *IEEE Transactions on Fuzzy Systems*, vol. 27, no. 4, pp. 646–658, 2019.
 - [31] S. Li, M. J. Er, and J. Zhang, “Distributed adaptive fuzzy control for output consensus of heterogeneous stochastic nonlinear multiagent systems,” *IEEE Transactions on Fuzzy Systems*, vol. 26, no. 3, pp. 1138–1152, 2018.
 - [32] H. K. Lam, H. Li, C. Deters, E. L. Secco, H. A. Wurdemann, and K. Althoefer, “Control design for interval type-2 fuzzy systems under imperfect premise matching,” *IEEE Transactions on Industrial Electronics*, vol. 61, no. 2, pp. 956–968, 2014.
 - [33] H. K. Lam and L. D. Seneviratne, “Stability analysis of interval type-2 fuzzy-model-based control systems,” *IEEE Transactions on Systems, Man, and Cybernetics, Part B (Cybernetics)*, vol. 38, no. 3, pp. 617–628, 2008.
 - [34] A. Boulkroune, M. Tadjine, M. M’Saad, and M. Farza, “Design of a unified adaptive fuzzy observer for uncertain nonlinear systems,” *Information Sciences*, vol. 265, pp. 139–153, 2014.
 - [35] M. H. Asemani and V. J. Majd, “A robust H_∞ non-PDC design scheme for singularly perturbed T-S fuzzy systems with immeasurable state variables,” *IEEE Transactions on Fuzzy Systems*, vol. 23, no. 3, pp. 525–541, 2015.
 - [36] S. Li and Z. Ge, “Fuzzy modeling and synchronization of two totally different chaotic systems via novel fuzzy model,” *IEEE Transactions on Systems, Man, and Cybernetics, Part B (Cybernetics)*, vol. 41, no. 4, pp. 1015–1026, 2011.
 - [37] S. Tong, X. Min, and Y. Li, “Observer-based adaptive fuzzy tracking control for strict-feedback nonlinear systems with unknown control gain functions,” *IEEE Transactions on Cybernetics*, vol. 50, no. 9, pp. 3903–3913, 2020.
 - [38] H. Zhang, Y. Mu, Z. Gao, and W. Wang, “Observer-based fault reconstruction and fault-tolerant control for nonlinear systems subject to simultaneous actuator and sensor faults,” *IEEE Transactions on Fuzzy Systems*, DOI: 10.1109/TFUZZ.2021.3098341, 2021.
 - [39] Y. Pan, Y. Wu, and H. K. Lam, “Security-based fuzzy control for nonlinear networked control systems with DoS attacks via a resilient event-triggered scheme,” *IEEE Transactions on Fuzzy Systems*, DOI: 10.1109/TFUZZ.2022.3148875, 2022.
 - [40] Y. Pan, Q. Li, H. Liang, and H. K. Lam, “A novel mixed control approach for fuzzy systems via membership functions online learning policy,” *IEEE Transactions on Fuzzy Systems*, DOI: 10.1109/TFUZZ.2021.3130201, 2021.
 - [41] T. Jia, Y. Pan, H. Liang, and H. K. Lam, “Event-based adaptive fixed-time fuzzy control for active vehicle suspension systems with time-varying displacement constraint,” *IEEE Transactions on Fuzzy Systems*, DOI: 10.1109/TFUZZ.2021.3075490, 2021.
 - [42] W. Sun, Y. Wu, and Z. Sun, “Command filter-based finite-time adaptive fuzzy control for uncertain nonlinear systems with prescribed performance,” *IEEE Transactions on Fuzzy Systems*, vol. 28, no. 12, pp. 3161–3170, 2020.
 - [43] Y. Li, T. Yang, and S. Tong, “Adaptive neural networks finite-time optimal control for a class of nonlinear systems,” *IEEE Transactions on Neural Networks and Learning Systems*, vol. 31, no. 11, pp. 4451–4460, 2020.
 - [44] Y. Li, Y. Liu, and S. Tong, “Observer-based neuro-adaptive optimized control of strict-feedback nonlinear systems with state constraints,” *IEEE Transactions on Neural Networks and Learning Systems*, DOI: 10.1109/TNNLS.2021.3051030, 2021.
 - [45] Y. Li, “Finite time command filtered adaptive fault tolerant control for a class of uncertain nonlinear systems,” *Automatica*, vol. 106, pp. 117–123, 2019.
 - [46] L. Xue, T. Zhang, W. Zhang, and X. Xie, “Global adaptive stabilization and tracking control for high-order stochastic nonlinear systems with time-varying delays,” *IEEE Transactions on Automatic Control*, vol. 63, no. 9, pp. 2928–2943, 2018.